UNIVERSITÀ DI PARMA

DOTTORATO DI RICERCA IN

"Neuroscienze"

CICLO XXXVIII

Visual and goal-related information are differentially encoded across distinct anatomical areas of the monkey ventrolateral prefrontal cortex

Coordinatore:

Chiar.mo Prof Luca Bonini

Tutore:

Chiar.mo Prof. Leonardo Fogassi

Chiar.mo Prof. Stefano Rozzi

Chiar.mo Prof. Marzio Gerbella

Dottorando: Claudio Basile

Anni Accademici 2022/2023 - 2024/25

Abstract

The lateral prefrontal cortex has been classically defined as an associative region involved in the so-called executive functions, such as guiding behavior based on abstract rules and mnemonic information. However, most neurophysiological studies on monkeys did not address the issue of whether distinct anatomical sectors of lateral prefrontal cortex play different functional roles. The main aim of this work is to study functional properties of neurons recorded from a large part of ventrolateral prefrontal cortex (VLPF) of two monkeys performing passive visual tasks and a visuo-motor task, and to map them on the anatomical areas defined on the basis of our recent parcellations. Our results show that some functional features are broadly distributed within VLPF, while others characterize specific areas. In particular, the temporal structuring of events and the general behavioral rule appear to be coded in all recorded areas, while each area differently contributes to the encoding of visual features and to the exploitation of contextual information for guiding behavior. Caudal VLPF areas, and especially caudal 12r, are characterized by a strong coding of visual information, both when passively presented or exploited for guiding behavior, while middle VLPF areas, and especially middle 46v, are rather more involved in the processing of contextual information for action organization. In this latter sector, visual stimuli/instructions appear to be encoded in a pragmatic format, that is, in terms of the associated behavioral outcome. Finally, area 45A and more anterior VLPF areas are characterized by a generally lower responsiveness to the employed tasks. Altogether, our findings indicate that caudal VLPF areas represent the first processing stage of visual input while middle VLPF areas primarily contribute to the selection and planning of contextually appropriate behaviors.

Authors' note

This thesis is based upon one study published during my PhD program, in which I am the first author:

"Encoding of visual stimuli and behavioral goals in distinct anatomical areas of monkey ventrolateral prefrontal cortex", published in *PLOS biology* in 2025. (https://doi.org/10.1371/journal.pbio.3003041)

Please note that, for the sake of readability, the supplementary information are shown in the appendix at the end of the thesis.

1. Introduction

1.1 Prefrontal cortex phylogeny and ontogeny

Cerebral cortical surface areas exhibit considerable variation across species, even within primates, as evident by the notable difference present between the average surface area per hemisphere amounting to 1,843 cm^2 for humans, 599 cm^2 for chimpanzees, 193 cm^2 for macaques, 9.6 cm^2 for marmosets (Van Essen et al., 2018).

The evolutionary origin of non-allometric prefrontal enlargement is traced back to the root of great apes, indicating that selection for changes in executive cognitive functions characterized both great apes and human cortical organization (Smaers et al., 2017). This process, initiated approximately 15-19 million years ago, reached its pinnacle in humans, where the prefrontal cortex constitutes 30% of the total cortical surface.

This growth was accompanied by a phylogenetic differentiation of cortical segments, which led to the development of several qualitatively and functionally unique regions (Carlén, 2017). Comparative histological studies of the frontal cortex and from other brain regions suggest that the internal organization and size of individual cortical areas are specialized among the hominoids - and it is this specialization and reorganization of specific areas that sets the various differences observed among species. An example of this specialization could be the relative volume of white matter underlying prefrontal association cortices, which is larger in humans than in great apes (Semendeferi et al., 2002).

One of the mechanisms considered to have been important in supporting this increase is neoteny, i.e. delayed brain development, a factor proposed to play a role in human's central nervous system development by influencing its maturation rate (Gould, 1977), as evidenced by humans' prolonged nervous and physical development relative to other primates; such extended development periods could allow for more extensive neural connections and therefore greater potential for cognitive complexity. Coherently with this hypothesis, Somel and colleagues (Somel et al., 2009) analyzed gene expression in the prefrontal cortices of both human and non-human primates throughout postnatal development, finding that humans exhibited a notable surplus of genes displaying neotenic expression. These data suggest that ontogenetic temporal differences in the prefrontal cortex (PF) of human and non-human primates can be considered to underlie existing

differences in cognitive maturation, in that delayed grey matter maturation in the human PF could prolong the period of neuronal plasticity associated with active learning, thus providing humans with more time, compared to non-human primates, to acquire knowledge and skills

1.2 Anatomical organization of the prefrontal cortex

In mammals' brain, PF covers the most anterior part of the frontal lobe. As mentioned above, the frontal lobe represents a considerable portion of the entire cortex, especially in humans. Table 1 shows how it is related to the rest of cortex in different primate species, in terms of extension; the various ratios are not so far from the human brain one, especially if we consider great apes such as gorillas, chimpanzees etc (Semendeferi et al., 2002).

The original cytoarchitectonic criterion used to define PF is his granularity (Walker, 1940). In fact, differently from posterior frontalmotor areas (Brodmann area 4) and secondary motor areas (Brodmann area 6, including the premotor cortex and the supplementary and presupplementary motor areas - SMA and Pre-SMA) that are agranular, that is lacking the granular IV layer, PF has a well-defined internal granular layer (IV), although it is not uniform across its different regions. Specifically, based on granularity, prefrontal cortices can be classified in real granular cortices (homotypic or eulaminated), with a thick IV layer, and dysgranular ones, with a thin IV layer (Carlén, 2017).

	Brodmann (1909)*	Blinkov & Glezer (1968)*	Semendeferi (2002)**
Human	36.3	32.8	37.7 (± 0.9)
Chimpanzee	30.5	22.1	35.4 (± 1.9)
Bonobo	ND	ND	34.7 (± 0.6)
Gorilla	ND	ND	35 e 36.9
Orangutan	ND	21.3	37.6 (± 1.1)
Gibbon	21.4	21.2	29.4 (± 9.8)
Macaque	ND	ND	30.6 (± 1.5)
Cebus	22.5	ND	29.6 e 31.5

Table 1: Relative size of the frontal cortex, expressed in percentage of the size of the entire cortex (Blinkov & Glezer, 1968; Brodmann, 1909; Semendeferi et al., 2002). **Surface of frontal cortex in percentage of surface of cortex of cerebral hemispheres. **Volume of frontal cortex in percentage of volume of cortex of cerebral hemispheres. ND, not available.*

According to Brodmann cytoarchitectonic classification, PF is mainly partitioned in three regions: the Lateral Prefrontal Cortex (LPF), the Medial Prefrontal Cortex (MPF) and the Orbitofrontal Cortex (OF). LPF is divided in two parts: the dorsolateral Prefrontal Cortex (DLPF), which includes lateral parts of areas 8 (including FEF) 9, 10, 11, 46, and the ventrolateral Prefrontal Cortex (VLPF), constituted by areas 44, 45 and 47. MPF faces off the medial surface of the contralateral PF and contains medial parts of areas 8, 9, 10, 11 and anterior cingulate areas 24, 32, 33. Finally, OF is placed above the eye sockets and includes areas 13, 47 and inferior parts of areas 10, 11, and 13.

The above described cytoarchitectural organization, together with the anatomical connectivity, is widely maintained also in macaque brain, the main animal model used in studying brains' structure and functions. Comparing the relative size of the frontal cortex in the primates' order (Table 1), we can see that human frontal cortex has the expected size for a primate of the human size (Semendeferi et al., 2002). In other words, there is not a real disproportion of human frontal cortex, relatively to what happens in great apes and in macaques; more plausible is the hypothesis of a specialization in relative white to grey matter volume, (especially on the left prefrontal cortex), shifting the focus to a concern of enhanced connectivity (Smaers et al., 2011).

The possibility to use a comparative approach between human and macaque brains requires the implementation of a nomenclature system that is identical, or strongly similar, for both human and macaque. The main system classically used to describe anatomical and neurophysiological results obtain in the macaque was that of Walker (Walker, 1940), which described the cytoarchitectural characteristics of the monkey brain with a numerical nomenclature similar to that used by Brodmann' for the human brain, although without a precise comparison from the cytoarchitectural point of view. A series of studies by Petrides and Pandya (Petrides & Pandya, 1999, 2002) raised the question about direct comparability among human and macaque's PF, observing that, as mentioned above, the majority of anatomical and physiological investigations concerning the macaque prefrontal cortex in the last 50 years have relied on numerical architectural nomenclature methods devoid of any comparative analysis between the cytoarchitecture of the human and macaque PF. These discrepancies pose a noteworthy challenge when comparing experimental findings derived from studies on non-human primates and humans, as the criteria for parcellating these areas in the two primate species are not always consistent. To address this issue, the authors suggested a PF subdivision that allows direct comparison between the macaque and human prefrontal cortices (Fig. 1). In particular, they demonstrated that, as in humans, the macaque PF can be subdivided into three principal divisions: orbital, medial and lateral, the latter of which is comprised both in humans and non-humans primates of areas 12, 47, 45 and 46 in the ventral part and areas 5, 8b and 9 in the dorsal portion (Petrides & Pandya, 1999, 2002).

This comparative approach allows for a more reliable comparison between experimental findings from non-human primates with results obtained in functional and structural neuroimaging of the human brain (Petrides et al., 2011).

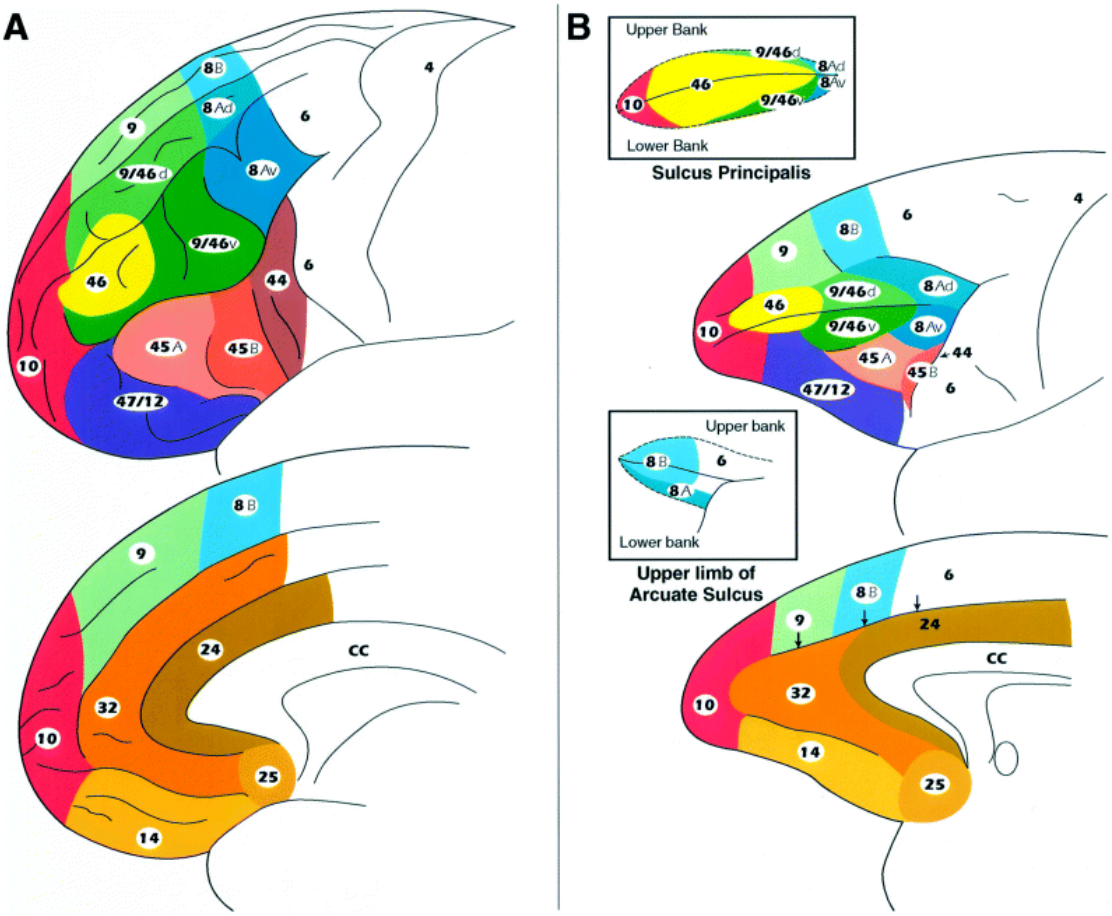

Figure 1: (A) Cytoarchitectonic maps of frontal lobe of the human and macaque monkey, (B) parcellation by Petrides and Pandya (Petrides & Pandya, 1999, 2002).

1.3 Connectional organization of the prefrontal cortex

From a connectional point of view, the PF constitutes a network of neocortical areas connected among themselves as well as with virtually all cortical sensory systems and motor systems and with many subcortical structures sending and receiving information to and from this zone . Regarding the cortical connections, Yeterian and collaborators (Yeterian et al., 2012) suggested that the connectivity of PF can be described from at least two points of view: local prefrontal connections and long-range association ones. Firstly, from a cytoarchitectonic perspective, two specific trends are recognized within the PF: a dorsal trend, which originates from medial prefrontal allocortex (the most primitive one, made of only three cortical layers) and includes medial and dorsolateral prefrontal regions, and a ventral trend, which starts from the caudal orbital allocortex and involves ventral and ventrolateral prefrontal regions. Local connectivity

seems to be consistent with this categorization, with a kind of local circuitry encompassing medial and dorsolateral portions of PF and another one characterizing ventrolateral and orbital portion. A similar organization can be observed in the case of long-range connections, indeed:

- medial and dorsolateral prefrontal regions are mainly connected to posterior dorso-medial visual and somatosensory association areas, together with caudo-dorsal auditory association areas, dorso-medial multimodal areas, and limbic areas.
- orbital and ventrolateral prefrontal regions are mainly connected to posterior ventro-lateral visual association areas, ventral somatosensory areas, and rostroventral auditory association areas, together with ventral multimodal and limbic areas.

Focusing on LPF, a series of recent connectional studies allowed to subdivide this region into three vertical portions, arranged in a rostro-caudal direction (Borra et al., 2017; Gerbella et al., 2017):

- The caudal portion (areas 8B, 8A, 8r, 8/FEF, 45A, 45B) is mainly connected to area LIP in the parietal lobe, FEF and SEF in the frontal lobe, and subcortical centres as the brainstem preoculomotor structures, the caudate nucles and the superior colliculus; it belongs to a network that seems to be involved in eyes' movements control (Borra et al., 2015; Gerbella et al., 2010, 2013; Saleem et al., 2014).
- The intermediate portion of LPF (areas 46d, 46v, 12r) belongs to a network involved in reaching and grasping movements; main connections include parietal areas like AIP, PFG, PG, premotor areas like F5, F6, F7, other cortical areas like SII, V6A, STS, insula, cingulate motor area 24 and subcortical structures such as the putamen (Borra et al., 2011, 2014; Gerbella et al., 2013, 2016, 2017; Saleem et al., 2014).
- The rostral-most portion (areas 9, 10, 46dr, 46vr) has a more intrinsic prefrontal connectivity, with other lateral prefrontal areas as well as orbital prefrontal areas and the frontal pole (Borra et al., 2011; Gerbella et al., 2013; Saleem et al., 2014).

1.4 Distributed coding in the lateral prefrontal cortex

The prominent local and long-range connectivity, described above is among the features that probably makes the PF a system useful to flexibly control behavior based on internal goals (Miller & Cohen, 2001). In particular, according to the integrative theory of PF function, proposed by EK Miller and JD Cohen, this part of the cortex seems to be involved in a quite peculiar role linked to the top-down control of behaviour. PF would generate robust and sustained activity that constitutes a bias signal facilitating the selection of neural pathways that represent precise

associations between certain inputs, both external and internal, and behavioural responses useful to fit with the available contextual information, keeping them active to achieve a certain goal (Miller & Cohen, 2001).

This functional model is in line with a series of classical studies suggesting that the LPF is involved, as a whole, in a series of processes that are the basis of the so-called “executive functions”, including working memory (Constantinidis & Procyk, 2004; Funahashi et al., 1989; Fuster & Alexander, 1971; Miller et al., 1996, 2018), attention (Boussaoud & Wise, 1993; Desimone & Duncan, 1995; Everling et al., 2002; Katsuki & Constantinidis, 2014) and rule coding (Hoshi et al., 2000; Muhammad et al., 2006; Wallis et al., 2001; White & Wise, 1999).

In line with this perspective, a recent body of research suggested the view that the LPF operates as part of a broader, distributed system that flexibly supports a wide array of cognitive demands. Central to this view is the multiple-demand (MD) network model, developed by John Duncan and colleagues based on a series of fMRI studies on human subjects (Crittenden & Duncan, 2014; Duncan, 2010; Duncan & Owen, 2000), which identifies a set of frontoparietal regions, including large portions of the LPF, that are consistently co-activated across a wide range of cognitively demanding tasks, in which a goal is achieved by a series of focused stages or sub-tasks. This network, and especially the LPF node, is thought to provide the neural substrate implementing general-purpose mechanism aimed at the “construction and control of such sub-tasks, with focus on the specific content of a current cognitive operation, rapid reorganization with changing context, and robust separation of successive task stages” (Duncan, 2010), which is fundamental for fluid intelligence and goal-directed behavior.

According to the adaptive coding hypothesis (Duncan, 2001), neurons within the LPF are capable of dynamically adjusting their tuning properties to represent task-relevant information depending on current behavioral goals and task demands. Rather than being hardwired to respond to specific stimulus types or task contexts, prefrontal neurons exhibit remarkable flexibility, selectively encoding rules, stimuli, or responses as needed. The authors further propose that distributions of cells carrying various types of information are overlapping withing LPF, prefrontal cells carrying various types of information are widely distributed across LPF, across the prefrontal cortex, but “these overlapping distributions might have different shapes and, in particular, different peaks or regions of maximal sensitivity” (Duncan, 2001).

This overall coding flexibility allows the LPF to function, as also mentioned above, as a kind of ‘mental workspace’ orchestrating different types of information and coordinating behavior in a context-sensitive manner (Duncan, 2001; Woolgar et al., 2011). Such dynamic, integrative

properties support the idea that the LPF, taken as a whole, contributes to a high-level control system essential for a wide variety of executive functions.

1.5 Action coding in the lateral prefrontal cortex

As described in the above sections, the LPF shows a connectivity pattern which involves various areas with motor functions, as the ones constituting parieto-premotor circuits, and subcortical structures like basal ganglia and cerebellum (Tanji & Hoshi, 2008). In particular, areas middle 46 and 12r of the VLPF have recently defined as constituting a prefrontal node the so called "lateral grasping network", a large-scale cortical network including parietal, premotor, temporal and prefrontal areas involved in the generation of hand actions (Borra et al., 2017; Gerbella et al., 2017). Although movement-related activity in VLPF neurons has been previously reported (Boussaoud & Wise, 1993; Funahashi et al., 1989; Hoshi et al., 1998; Kubota & Funahashi, 1982; Kubota & Niki, 1971; Niki, 1974; Niki & Watanabe, 1976; Tanila et al., 1992), it is generally difficult to determine whether such activity reflects motor execution per se or rather perceptual and attentional processes associated with action selection, especially since the elicited responses were often tied to the encoding of specific task rules.

More recently, Rozzi and coworkers reported the presence of movement-related activity in the VLPF, especially in the intermediate part of area 46v, during reaching-grasping actions in different behavioural contexts (Simone et al., 2015). In this study, neural activity was recorded while the monkeys performed a visuomotor task in which a green cue instructed them to reach and grasp different objects (Motor condition), while a red cue instructed them to or simply to observe them; in addition to this main task, two control motor conditions have been used: in the first one, the monkey movement was based exclusively on mnemonic information, since the object was not visible; in the second one, the grasping action was performed in a naturalistic context, since the monkey had to simply execute it without any rule constraint.

The main result of this study is the demonstration that VLPF neuronal activity is not only dependent on the learned relationship between instruction and motor output but more specifically to the execution of grasping actions. In other words, it demonstrated the presence of grasping-related neurons in this VLPF sector. Most of these VLPF grasping-related neurons have their peak discharge during movement or holding phase, and, in line with this observation, the strongest

discharge of the entire population of these neurons, in terms of mean firing rate, is reached at the beginning of object pulling.

Only a small subpopulation of neurons studies in this work showed grip selectivity, some of which showed an activation during the simple observation of objects, unlike what is observed in premotor area F5 and in the parietal area AIP, where the congruence between visual and motor preferences is typical. The general activity of this movement-related population of neurons was not strongly influenced by the different conditions in which grasping was performed (presence vs absence of visual control, naturalistic vs learned rules, current vs mnemonic information). Based on these results, the authors hypothesized that, differently from the main nodes of the grasping network, this VLPF node should not be directly involved in operating visuo-motor transformations but could play a more general role in encoding the action goal, such as to take possession of a given object (Simone et al., 2015). In other words, this study demonstrates that VLPF neuronal activity is not specifically dependent on the presence of a learned relationship between instruction and motor output as previously thought.

Interestingly, two-thirds of the movement-related VLPF neurons recorded in this study respond not only during the movement phases of the Go condition but also in the task phases preceding movement, in both conditions (for example during the various phases of the NoGo condition, in which the monkey had to simply observe the object). Some of these neurons, in particular, respond to cue appearance, which instructs the monkey about which condition to perform, most of them without showing any preference for one of the two conditions, defined as Motor and Visual ones.

A third of the movement-related neurons respond during the presentation of the object, most of which showing a preference for the Motor condition. Cue appearance and object presentation are two task phases in which visual information can be exploited to generate behavioural goals, but, however, these results suggest that the presence of a graspable object is a more effective stimulus than the type of cue in modulating the activity of VLPF movement-related neurons.

A high percentage of VLPF movement-related neurons respond during the task phases immediately preceding the movement onset of the Motor condition: among them, many show a condition preference starting from object presentation. In agreement with studies describing VLPF role in movement planning (Averbeck et al., 2002; Funahashi et al., 1993; Quintana & Fuster, 1992; Shima et al., 2007; Tanji & Hoshi, 2008; Yamagata et al., 2012), as also mentioned above, this peculiar activity could represent the maintenance of action goal representation.

To understand how VLPF links abstract rules, object features and the instructed behaviour, and in particular to describe the format in which VLPFC neurons encode instructions and behaviours, Rozzi and colleagues (Rozzi et al., 2023) analysed the entire population of neurons recorded in the aforementioned study of Simone and colleagues (Simone et al., 2015), focusing their attention on the temporal dynamics of the various populations with respect to the different phases of the visuomotor task (Rozzi et al., 2023). One of the main results is that the most relevant factor in modulating the neural discharge is the behavioural condition (the two conditions, instructed by a green or red cue respectively, are defined here as Action and Inaction). About 20% of the recorded units can be classified as “condition-dependent” neurons; the condition preference of this population of neurons is different among the task phases, both in terms of neurons numerosity and of average population discharge. Specifically, these neurons show a clear preference for the appearance of the red cue (Inaction condition); a possible interpretation is that when the red cue is presented, the associated behaviour, that is keeping the hand on the starting position and fixating the object until reward delivery, is already set and no more information useful to choose the right behavioural output is necessary.

During object presentation, the preference of “condition-dependent” neurons inverts in favour of the Action condition and is maintained until the object pulling (Behavioural response phase). This phenomenon is in line with the fact that in the Action condition, object presentation constitutes a relevant task phase in which information about the object allows to progress from the encoding of the general behavioural goal to the planning of the specific motor program to be executed. Another interesting analysis performed in this study is the decoding analysis, that was carried out on the two cue-responsive condition-dependent populations (here defined as action-related and inaction-related neurons); this analysis led to the hypothesis that these neurons encode the instruction in a “pragmatic format”. In particular, it showed that, the activity patterns observed in the initial phases of the task is similar to that observed in the final phases. These results suggest that Cue-related neurons encode the instructions in terms of behavioural outcomes.

The second factor considered in this study was the type of object, that seems less effective in conditioning neural discharge. Nonetheless, about 10% of neurons activate during the presentation of the object (Presentation-responsive neurons) has some type of object preference, and decoding analysis carried out on the sub-population composed by Action-related neurons which have an object preference reveals a similar activity pattern for Presentation and Behavioural-response phases; this suggest that: 1) this population could functionally resemble that constituted

by visual and visuomotor neurons of the parieto-premotor grasping circuit; and 2) the object coding in the Action condition could be related to motor program implementation.

These data led the authors to propose a “pragmatic hypothesis”, according to which LPF neurons encode the goal of a wilful action by representing some crucial events, as grasping/holding or keeping fixating without moving and getting the reward, which are representative of the goal’s outcome. According to this view, Action related neurons’ activity during Presentation shares a similar pattern with activity in the Behavioural period; in addition, Action-related neural activity abruptly decreases when the object is grasped and pulled. Plausibly, during Presentation phase there is enough information to accomplish the task and then, to represent the goal achievement. The activity of the less represented population of Inaction-related neurons, instead, decreases significantly only when the reward is delivered. This kind of goal representation would be useful in keeping active some sensory-motor representations of actions meanwhile selection, programming and execution processes are unfolding, through a modulation of parieto-premotor grasping neurons connected to VLPF (Miller & Cohen, 2001).

1.6 Encoding of visual properties in the lateral prefrontal cortex

Many neurons in the lateral prefrontal cortex (LPF) show responses to visual stimuli, typically interpreted either in terms of categorical encoding or as the result of learned associations between stimuli and subsequent behaviors (Freedman et al., 2001; Saga et al., 2011; Seger & Miller, 2010; Yamagata et al., 2012). In the latter case, these responses are often followed by sustained, memory-related activity (Funahashi et al., 1989; Funahashi & Andreau, 2013; Fuster, 2015; Levy & Goldman-Rakic, 2000).

It is generally accepted that responses of prefrontal neurons to visual stimuli may relate to their physical and/or spatial properties. In particular, based on this distinction, the LPF has been functionally divided into two sectors: a dorsal part (DLPF), primarily involved in processing spatial aspects of visual information, and a ventral part (VLPF), more associated with the analysis of object features (Levy & Goldman-Rakic, 2000; Passingham et al., 2000; Wilson et al., 1993). This broad functional subdivision aligns with neuroanatomical data showing that the dorsal sector is mainly connected to the posterior parietal cortex, while the ventral sector is linked to inferotemporal areas (Romanski, 2004)

However, this sharp dichotomy has been challenged by electrophysiological studies using visual stimuli that vary in location, shape, and color (Constantinidis & Qi, 2018; Riley et al., 2017). While confirming that the LPF exhibits greater selectivity for spatial location, these studies did not find a strong and consistent preference of the VLPF for the physical features of stimuli. Moreover, spatial and semantic specificity appears more pronounced in posterior regions of both the DLPF and VLPF, whereas moving rostrally, neural responses become increasingly abstract and tuned to behavioral task demands (Constantinidis & Qi, 2018; Riley et al., 2017).

A series of recent studies by Rozzi and collaborators investigated VLPF role in processing visual stimuli and modulating responses based on behavioral context and observed action (Rozzi et al., 2021; Simone et al., 2017). In the first study (Simone et al., 2017) the authors found that a population of VLPF neurons responds to the observation of biological movements, particularly goal-directed actions. Many of these neurons displayed a preference for the agent performing the action, with actions performed by monkeys being most frequently encoded by selective neurons. Critically, the study investigated the nature of this neural coding by obscuring parts of the observed movements. The results indicated that the response of the majority of VLPF neurons was not affected by the partial occlusion of the observed movement, suggesting that these VLPF neurons encode a higher-order representation of the observed action, rather than merely a simple visual description of its features.

In a subsequent study (Rozzi et al., 2021), the authors primarily investigated the visual responses of VLPF neurons when monkeys passively observed static images and how these responses changed when the objects became targets of grasping actions. They found that roughly half of the recorded VLPF neurons were visually responsive during passive observation of static images. A subset of these (about 10%) showed selectivity for specific stimuli, with the majority responding uniquely to a single stimulus. Interestingly, there was no clear evidence of "passive categorical coding", as would be suggested by a similar response to all stimuli representing food, or faces. However, some selective neurons responded to stimuli from different categories that shared common features, such as shape and orientation (e.g., cylinder and banana). These visually responsive neurons were broadly distributed across areas 45A, 46v, and 12, without clear anatomical segregation based on stimulus types or categories. Population analysis revealed that selective neurons exhibited a prolonged, sustained discharge throughout the entire stimulation period, unlike unselective neurons, suggesting a role in maintaining attention on the target.

Furthermore, Rozzi and collaborators (Rozzi et al., 2021) demonstrated that VLPF neuronal visual responses to objects are frequently modulated by the task conditions under which the object

is observed. Indeed, about half of the tested neurons showed differential responses to the same objects based on whether the monkey was simply observing it (Visual condition) or had to act or withhold acting on them (Action and Inaction conditions, respectively). The strongest neural responses were observed when the object was the target of an action (Action condition). This suggests a strong link between visual responses and the monkey's intended action, even if the neuron itself doesn't directly control the movement. The population analysis confirmed this, showing the highest discharge for objects in the Action condition, an intermediate response for the Inaction condition, and the weakest for the Visual condition, indicating that higher behavioral relevance of an object leads to a stronger prefrontal neuron response.

Overall, these findings underscore the VLPF's role in integrating visual information with context to guide behavioral responses, understand the actions of others, and potentially even discriminate between self and other actions.

1.7 Connectional and functional specificity of the areas constituting the VLPF

A series of recent studies carried out Luppino and coworkers allowed to subdivide the VLPF into several areas, modifying the initial parcellation of Walker and the parcellation proposed by Petrides and Pandya, described above, by using a multimodal architectonic and connectional (Borra et al., 2011; Gerbella et al., 2007, 2013). The areas identified in these studies are:

- Areas 8-FEF, 8r, 45B, located inside and near the arcuate sulcus.
- Areas 45A, 12r (further subdivided in rostral, middle, and caudal parts), 12l, located in the ventral convexity.
- Area 46v (further subdivided in rostral, middle, and caudal parts), located inside and around the ventral bank of principal sulcus.
- Area 10, located in the frontal pole.

This multimodal approach highlighted that the boundaries between these areas change gradually, generating both a rostro-caudal and dorso-ventral gradient of areal differentiation within VLPF. In this section, the currently available evidence related to the functional and anatomical features of the different VLPF areas that are studied in this work will be briefly described.

Area 45A

Most of area 45A has been classically considered as part of a larger cortical sector which corresponded mainly to Walker's area 12; connectional and architectonic studies of the last years collected enough evidence to distinguish area 45A from all others VLPF regions (Borra et al., 2015; Gerbella et al., 2007, 2010; Saleem et al., 2014). In particular, these studies showed that area 45A is strongly connected to the neighbouring caudal VLPF regions (caudal 12r and caudal 46v), as well as with several oculomotor cortical and subcortical centres, such as areas 8-FEF, 45B, 8r, and the superior colliculus, and to more rostral areas, as frontopolar area 10 and rostral 46d (also connected to dorsal 8-FEF). In addition, among all VLPF areas, 45A was shown to be characterized by the fact that it's a target of temporal input from superior temporal polysensory area STP and rostral and caudal auditory parabelt areas (Gerbella et al., 2010).

Functional studies have shown that neurons responsive to visual, auditory, or bimodal combined stimuli have been found in a cortical sector which involves 45A and caudal 12r, and fMRI data showed that area 45A is active in correspondence of the observation of faces and actions (Romanski, 2007; Romanski & Averbeck, 2009; Romanski L.M., 2004; Tsao & Livingstone, 2008; Nelissen K. et al., 2005). In addition, as the connectivity with cortical and subcortical oculomotor centres suggest, area 45A is active in correspondence of the execution of saccades, during tasks in which is required to do a visual search or spatial attention tasks (Baker et al., 2006; Premereur et al., 2015; Wardak et al., 2010; Caspari et al., 2015).

Connectional and functional data indicate that area 45A could play a complex role, substantially linked to the control of gaze direction during the social communication behaviour and according to some authors in analogy with language-related human area 45 (Romanski, 2007; Romanski L.M., 2004; Sugihara et al., 2006; Petrides & Pandya, 2002).

Area 12r

From a connectional point of view, area 12r exhibits a rostro-caudal gradient of connections which allows to subdivide it into three different subregions (Borra et al., 2011; Saleem et al., 2014):

- A caudal part, here defined as caudal 12r, shows connection with neighboring frontal oculomotor areas and with inferotemporal regions.
- A middle part, here defined as middle 12r, showing connections with other lateral prefrontal and orbitofrontal regions, as well as with inferior and opercular parietal areas, ventral premotor hand-related areas and inferotemporal areas.

- A rostral part, here defined as rostral 12r, primarily showing connections with other lateral prefrontal and orbitofrontal areas, as well as weak connections with the upper bank of the STS and cingulate area 24..

Considering the functional features of these regions, it has been observed that VLPF neurons recorded in a region ventral to area 46v and including caudal and middle 12r are involved in coding the identity or features of objects (Asaad et al., 1998; Wilson et al., 1993) as well as in behavioral tasks in which object identity plays a key role (Mishkin & Manning, 1978; Passingham et al., 2000; Wang et al., 2000) and in visual categorization (Freedman et al., 2001; Miller et al., 2002). Furthermore, electrophysiological investigations by Romanski and colleagues (Romanski, 2004, 2007; Romanski & Averbeck, 2009) show that a region composed by area 45A and a portion of the caudal area 12r contains neurons responsive to visual communication stimuli; this responsiveness likely stems from input to this area from higher-order multisensory anterior temporal regions. Additionally, fMRI data on human subject revealed an activation of a similar region during the observation of faces (Tsao & Livingstone, 2008) and other's actions (Nelissen et al., 2005). Finally, middle 12r, together with middle 46v (described below), seems to contribute to the formation of multimodal representations of the behavioural target and to the coding of contextual information in order to select and guide object-oriented hand actions (Bruni et al., 2015), also hosting movement-related neurons responding both to actions performed within a structured task or in naturalistic conditions (Bruni et al., 2015; Simone et al., 2015).

Area 46v

Area 46v, as described above for area 12r, can also be subdivided into three rostro-caudal segments, based on their connectional properties (Gerbella et al., 2013; Saleem et al., 2014):

- The caudal part, here defined as caudal 46v, connected almost exclusively to frontal and parietal oculomotor areas such as areas 8-FEF, 8r, 45b, the supplementary eye fields (SEF) and inferior parietal area LIP.
- A middle part, here defined as middle 46v, characterized by connections to parietal and frontal arm/hand-related areas F5a, SII and inferior parietal area AIP
- A rostral part, here defined as rostral 46v, showing extensive intra-prefrontal connectivity which involves not only ventrolateral and orbitofrontal areas, but also dorsolateral ones, and also connection to cingulate area 24.

From a functional point of view, numerous studies showed significant activation of neurons hosted within caudal 46v during tasks requiring oculomotor responses (Boch & Goldberg, 1989;

Ichihara-Takeda & Funahashi, 2007). Neurons in this region are also characterized by pre-saccadic activity (Funahashi et al., 1991) and by an encoding of visual cue location or saccade direction in spatial working memory tasks (Funahashi et al., 1993); these neurons are also modulated by the inactivation of area LIP during the performance of oculomotor delayed responses (Chafee & Goldman-Rakic, 2000).

Activity of middle 46v neurons seems to be linked to the encoding of the final goal representations of sequential actions, the consequences of actions and the different phases of a behaviour, suggesting a role in governing goal-oriented sequential behavior and in encoding information representing multiple phases of behavioral actions (Saga et al., 2011; Saito et al., 2005; Shima et al., 2007). In line with these observations and with the above described connectional data, it has been demonstrated that, as mentioned above, middle 46v also hosts, together with middle 12r, multisensory neurons that appear to encode a behavioral decision independently from the sensory modality of the stimulus (Bruni et al., 2015), as well as neurons showing a response during the execution of object-oriented hand actions based on contextual information or also in natural conditions (Bruni et al., 2015; Simone et al., 2015).

1.8 Aim of the study

Altogether, the above descrived data indicate that some functional and anatomical features are broadly distributed along VLPF, while others appear to be localized in specific sub-regions/areas. This is in line with theoretical models focused on describing the adaptability of functional properties in the prefrontal cortex (e.g. adaptive coding and multiple demand framework models, (Assem et al., 2020; Duncan, 2001, 2010; Kadohisa et al., 2023). In particular, Duncan and coworkers observe that, although neurons encoding different types of information (e.g. location and object) are broadly distributed across LPF, different subregions are characterized by a maximal sensitivity to one specific type of information. They propose that the use of complex tasks allows one to identify the broader distribution of properties, while low demanding behavioral paradigms could highlight regional specialization.

The general aim of this work is to map the distribution of VLPF neuronal properties based on the hypothesis that functional specialization depends on the specific connections that characterize each anatomical area. To achieve this aim: 1) we recorded single neuron activity in monkeys performing different tasks investigating how visual information is either passively

processed or exploited to guide a behavior involving the decision to produce or withhold grasping actions; 2) we analyzed the recorded data with reference to the anatomical parcellations produced by our group (Borra et al., 2011; Gerbella et al., 2007, 2010, 2013).

2. Materials and Methods

2.1 Subjects and ethical approvals

The experiment was carried out on two female Rhesus monkeys (Macaca mulatta, M1, M2) weighing about 4 kg. The animals have been previously employed in a series of experiments, whose results have already been published (Rozzi et al., 2021, 2023; Simone et al., 2015, 2017). All methods were carried out in accordance with the European (2010/63/EU) and the ARRIVE guidelines. The experimental protocols, the animal handling, and the surgical and experimental procedures complied with the European guidelines (2010/63/EU) and Italian laws in force on the care and use of laboratory animals, and were approved by the Veterinarian Animal Care and Use Committee of the University of Parma (Prot. 78/12 17/07/2012) and authorized by the Italian Ministry of Health (D.M. 294/2012-C, 11/12/2012).

2.2 Training and surgical procedures

The monkeys were first habituated to seat on a primate chair and to familiarize with the experimental setup. At the end of the habituation sessions, a head fixation system (Crist Instruments Co. Inc.) was implanted. Then, the monkeys were trained to perform the tasks described below. After completion of the training, a recording chamber (32x18 mm, Alpha Omega, Nazareth, Israel) was implanted on the ventrolateral prefrontal cortex (VLPF), based on MRI scan. All surgeries were carried out under general anesthesia (ketamine hydrochloride, 5 mg/kg, i.m. and medetomidine hydrochloride, 0.1 mg/kg, i.m.), followed by postsurgical pain medication.

2.3 Experimental apparatus

During training and recording sessions, the monkeys seated on the monkey chair with the hand contralateral to the hemisphere to be recorded on a resting position, located 9 cm in front of the abdomen. A monitor was positioned in front of the monkey, to present the visual stimuli used in the passive tasks (Picture and Video tasks, see below). The monitor, with a resolution of 1680x1050 pixel, was positioned at 54 cm from the monkey's face, and its geometrical center was located at the height of monkey's eyes. A laser spot could be projected on the center of the screen as a fixation point. A phototransistor was placed on the monitor in order to provide the onset and offset of the visual stimuli.

During the Visuo-Motor task, a box containing three objects was positioned at 22 cm from the monkey's chest. The opening of a small door (7x7 cm) in the frontal panel of the box at the height of monkey's eyes allowed to present the three objects, one at the time. Two laser spots (instructing cues) of different colors (green and red) could be projected onto the box door or onto the object, signaling the task conditions and phases.

2.4 Behavioral paradigms and stimuli

Picture task

The Picture task corresponds to the *Visual task* described in (Rozzi et al., 2021). Briefly, to evaluate the response of VLPF neurons to the observation of static visual stimuli, 12 different images (6°x6°; see below) were presented, while the monkeys kept their gaze within a 6°x6° fixation window centered on the stimulus. Fig 2A shows the sequence of events occurring during each trial. The monkeys were required to keep their hand on the resting position; if this was accomplished, the trial started, and the fixation point (red laser spot) was turned on, and they had to fixate it for a randomized time interval (500-900 ms). If they kept fixation for this period of time, the fixation point turned off and one of the images was presented for 600 ms, centered on the fixation point. The monkeys had to observe it (without breaking fixation) throughout the presentation period. Then, the image disappeared, the fixation point turned on again for a randomized period (500-900 ms) and the monkeys had to keep fixation on it.

The trials were accepted as correct, and the monkeys were rewarded, if they kept their eyes within the fixation window for the duration of each phase of the task and did not release the hand from the resting position. Discarded trials were repeated at the end of the sequence to collect at least 10 presentations for each stimulus. The order of stimuli presentation was randomized.

The 12 stimuli (Fig 2A) belong to 4 different semantic categories:

- Graspable solids (pictures of the objects employed in the motor task described in : cube, cylinder, sphere);
- Fruits: apple, banana, peanut;
- Faces: human face, monkey face, sketchy drawing of a face;
- Laboratory furniture, geometric, but not graspable: shelf, monitor and clock.

The stimuli were homogeneous for luminance. Note that the fruits and solids could evoke similar affordances (apple and cube: power grip; banana and cylinder: finger prehension; sphere and peanut: precision grip).

Video Task

The Video task corresponds to that described in (Simone et al., 2017). In order to evaluate the response of VLPF neurons to observation of dynamic visual stimuli, we displayed videos (12°x12°) showing several biological stimuli and object motion (see below), while the monkey maintained fixation within a 6°x6° fixation window centered on the video. The sequence of events occurring during each trial is the same as in the Picture task (see Fig 2B), but the stimuli were presented for 1800 ms. The criteria employed for trial acceptance were the same as in the Picture task (see above).

Discarded trials were repeated at the end of the sequence in order to collect at least 10 presentations for each stimulus. The order of stimuli presentation was randomized.

The construction of the set of video stimuli was devised so to present to the monkey goal-related or non-goal-related actions, different agents and presence or absence of an object. Specifically, the 6 stimuli were the following (Fig 2B):

- Monkey grasping in first person perspective (*MGI):* a monkey right forelimb enters into the scene from the lower border of the video, reaches and grasps a piece of food located in the center of it, and lift it toward itself (only the initial phase of this latter movement is visible). The observed forelimb is presented as if the observing monkey was looking at its own forelimb during grasping.

- Monkey grasping in third person perspective (*MGIII):* a monkey, located in front of the observer, with its left forelimb reaches and grasps a piece of food located in the center of the video, and brings it toward itself.

- Human grasping (HG): a human actor, located on the right of the video reaches, grasps and lifts an object, located in the center of the video, with his right forelimb.

- Human mimicking (HM): a human actor, located on the right of the video, performs the pantomime of the same action shown in HG, without the object.

- Biological movement (BM): a human actor located on the right of the video extends his right forelimb, with the hand open, to reach the central part of the screen. No object is present.

- Object motion (OM): an object is presented in the center of the screen and moves along the same trajectory as in HG. This stimulus was obtained by removing the agent from HG, in order to have same stimulus kinematics as in HG.

In the videos the agents' faces were not shown in order to avoid the possible influence of neural responses due to face presentation.

Visuo-Motor task

The Visuo-Motor task is the same described in (Rozzi et al., 2023; Simone et al., 2015). Briefly, the task consisted of two basic conditions: Action and Inaction (Fig 2C). Each trial started with the monkeys' hand on the starting position. Then, one of the two instructing cues (green=Action condition; red=Inaction condition) was turned on and projected onto a closed box door, placed in front of the monkeys. In both conditions, the monkeys had to maintain fixation within a 6°x6° fixation window centered on the instructing cue for a randomized time interval (500-1100 ms). Then, the box door opened allowing the monkeys to see one of three objects.

In the Action condition, during object presentation, the monkeys had to maintain fixation with the green cue still on, projected onto the object. After a randomized time (700 to 1100 ms), the green cue turned off (Go signal), instructing the monkeys to reach for, grasp the object and pull it.

In the Inaction condition, the trial unfolding and the events timing was the same as in the Action condition till the red cue turned off, after which the monkeys were required to keep fixation

for a further 600 ms period, refraining from acting. The order of presentation of both objects and conditions was randomized.

If the monkeys correctly performed a trial, the reward was delivered at the end of it. A trial was discarded when one of the following types of error occurred: 1) releasing the hand from the resting position before reward delivery in the Inaction condition or before the Go signal in the Action condition; 2) breaking fixation before reward delivery in the Inaction condition or before the Go signal in the Action condition; 3) failing to reach and grasp the object; 4) grasping the object with an incorrect prehension. Discarded trials were repeated at the end of the sequence to collect at least 30 correct trials for condition (10 trials x 3 objects).

2.5 **Recording techniques, task events acquisition and microstimulation**

Neuronal recordings were performed by means of a multi-electrode recording system (AlphaLab Pro, Alpha Omega Engineering, Nazareth, Israel) employing a maximum of eight glass-coated microelectrodes (impedance, 0.5-1 MΩ) inserted through the intact dura. The microelectrodes were mounted on an electrode holder (MT, Microdriving Terminal, Alpha Omega) allowing electrodes displacement, controlled by a dedicated software (EPS; Alpha Omega). The MT holder was directly mounted on the recording chamber. Neuronal activity was filtered, amplified, and monitored with a multichannel processor and sorted using a multi-spike detector (MCP Plus 8 and ASD, Alpha Omega Engineering). Spike sorting was performed using the Off-line Sorter (Plexon, Inc, Dallas TX, USA). During each recording session, electrodes were inserted one after the other inside the dura until the first neuronal activity was detected for each of them. Each electrode was then deepened into the cortex independently one from the other, in steps of 500 µm until the depth at which the border between gray and white matter was reached (see (Rozzi et al., 2008) for a similar procedure). At each site, multiunit and single-unit activities were recorded for subsequent analyses. In the present study, we considered the activity recorded at three levels of depth (500, 1000, 1500 µm). The experiment was controlled by a homemade Labview software. Digital output signals determined the onset and offset of laser spots, image/videoclip presentation, opening of the door and reward release. Contact-detecting electric circuits provided the digital signals related to monkey hand contact and release of the resting position and the beginning and end of object pulling.

In order to identify the sector where eye movements can be elicited by intracortical microstimulation, the recording microelectrodes were also used for delivering intracortical monophasic trains of cathodic square wave pulses, through a constant current isolator (World Precision Instruments, Stevenage, UK) with the following parameters: total train duration, 50 ms or, when no response was elicited, 100 ms; single pulse width, 0.2 ms; pulse frequency, 330 Hz. The stimulation started with a current intensity of 100 μA that was decreased until threshold definition and was controlled on an oscilloscope by measuring the voltage drop across a 10 KΩ resistor in series with the stimulating electrode.

Eye movements were recorded using an infrared pupil/corneal reflection tracking system (Iscan Inc., Cambridge, MA, USA) positioned above the box. Sampling rate was 120 Hz.

2.6 Histology, reconstruction of the recorded area and identification of the regions of interest on the basis of architectural and connectional data

Before sacrificing the animals, electrolytic lesions (10 μA cathodic pulses per 10 s) were performed at known coordinates at the external borders of the recorded region. After one week, each animal was anaesthetized with ketamine chloride (15 mg⁄kg i.m.), followed by an i.v. lethal injection of pentobarbital sodium and perfused through the left cardiac ventricle with buffered saline, followed by fixative. The brain was then removed from the skull, photographed, frozen and cut coronally. Each second and fifth section (60 μm thick) of a series of five were stained using the Nissl method. The locations of penetrations were then reconstructed on the basis of electrolytic lesions, stereotaxic coordinates, depths of penetrations and functional properties. More specifically, penetrations deeper than 3000 μm located inside the Arcuate sulcus and Principal Sulcus were used in order to localize the posterior and dorsal border of VLPF, respectively.

In order to define anatomical areas in the recorded brains, we performed a parcellation relying on previous architectonical and connectional studies from our lab (Borra et al., 2011; Gerbella et al., 2007, 2010, 2013). In those studies, we first defined the architectonic borders of areas 8FEF, 8r, 45A, 45B, 46v, and 12r and, subsequently, we injected neural tracers in these areas on 12 monkeys (see Table S1); the different pattern of connections observed after each injection confirmed the architectonic borders and allowed to further subdivide areas 46v and 12r in three additional sectors. In the present work, we superimposed the areas and sectors identified in the

above-mentioned studies onto the histological reconstructions of the two recorded brains, by warping both the architectonic maps and the locations of the various injection sites used to characterize the connectivity of each area. Specifically, this warping was performed using a non-linear transformation procedure (for details see (Nelissen et al., 2011)) based on specific anatomical anchor points: the anterior and posterior tips of the principal sulcus, the spur of the arcuate sulcus, the tips of the superior and inferior limbs of the arcuate sulcus, the tips of the superior and inferior prefrontal dimples, and the orbital reflection at the level of the lateral orbital sulcus.

In addition, we defined an oculomotor prearcuate sector by using microstimulation and recording of saccade-related neuronal activity. More in details, concerning microstimulation, oculomotor sites were those in which saccadic eye movements could be elicited with currents lower of or equal to 60 μA, with a train duration of 50 or 100 ms; concerning single neuron recordings, we described saccade-related activity by aligning the neuronal discharge with the moment in which the eyes reached a fixation target. This region, overlapping the location of areas 8 and 45B, has been excluded from further analyses.

The location of our recording chamber allowed us to record only from a small number of sites falling in areas rostral 46v and rostral 12r, especially in M2, thus we pulled together the data obtained from these areas and named this region *rostral sector*.

2.7 Analysis of single neurons responses

The digital signals representing the different task events, described above, were employed to align neuronal activity and to create the response histograms and data files used for the statistical analyses described in the subsequent paragraphs.

Picture task

We recorded neuronal activity for at least 120 successful trials, 10 for each stimulus. For the statistical analysis, two epochs were defined (see (Rozzi et al., 2021)): 1) *Baseline*: 500 ms preceding stimulus presentation, during which the monkey was looking at the fixation point; *2*) *Presentation*: the first 500 ms of image presentation.

Single-neuron responses were statistically evaluated by means of a 2X12 ANOVA (Factors: Epoch, Stimulus, $p<0.01$) followed by Newman-Keuls post hoc tests.

A neuron was considered as task-related when the 2X12 ANOVA revealed: 1) a significant main effect of the Epoch factor ($p<0.01$) and/or 2) a significant interaction effect (Epoch x Stimulus, $p<0.01$), with the post-hoc tests showing a significant difference between at least one *Presentation* epoch of one image and its corresponding *Baseline epoch*. Task-related neurons were classified as *selective* when the 2X12 ANOVA revealed a significant Interaction effect and the post-hoc test showed a significant difference among the activity recorded in the *Presentation epoch* of one image and that of its corresponding *Baseline epoch* as well as a significant difference between the activity recorded in the *Presentation epoch* of that image and the *Presentation epoch* of at least another image. Neurons were classified as *unselective* when the statistical test revealed a significant Main effect of the Epoch factor and/or a significant Interaction effect, and the post-hoc test did not show any difference among the activities recorded in the *Presentation* epochs of the 12 images.

Video task

We recorded neuronal activity for at least 60 successful trials. For the statistical analysis, three epochs were defined (see (Simone et al., 2017)): 1) *Baseline*: 500 ms before the beginning of the videos, during which the monkey was looking at the fixation point; 2) *Video Epoch 1*: the first 700 ms of the videos (except for MGI, where, because of the fastest arm movement, the epoch lasted 500 ms); 3) *Video Epoch 2*: the subsequent 700 ms of the videos. Note that Epoch 1 includes the context of the scene and the beginning of the forelimb movement, while Epoch 2 includes the hand-object contact in the case of action and the end of movement/object motion in all other videos.

Single-neuron responses were statistically evaluated by means of a 3X6 ANOVA (Factors: Epoch, Stimulus, $p<0.01$) followed by Newman–Keuls post hoc tests.

A neuron was considered as task-related when the 3X6 ANOVA revealed: 1) a significant main effect of the Epoch factor ($p<0.01$), with post-hoc tests indicating a significant difference between at least one of the two *video epochs* and the baseline and/or 2) a significant interaction effect (Epoch x Stimulus, $p<0.01$), with post-hoc tests showing a significant difference between at least one of the *video epochs* of one video and the corresponding *baseline* epoch.

Task-related neurons were classified as *selective* when the 3X6 ANOVA revealed a significant Interaction effect and the post-hoc test showed a significant difference among the activity recorded in one of the two *Video epoc*hs of one video and that of the corresponding *Baseline epoch* as well as a significant difference between the activity recorded in one of the two *Video epochs* and that recorded in the same epochs of at least another video. Neurons were classified as

unselective when the statistical test revealed a significant Main effect of the Epoch factor and/or a significant Interaction effect, and the post-hoc test did not show any difference among the activities recorded in the *Video epochs* of the 6 videos.

Visuo-Motor task

We recorded neuronal activity for at least 60 successful trials (thirty per condition, 10 for each object). For statistical analysis of the neural activity, nine epochs have been defined (see (Rozzi et al., 2023)), based on the digital signals: 1) Baseline: from 750 ms to 250 ms before the onset of the instructing cue; 2) Pre-cue: 250 ms preceding the onset of the instructing cue; 3) Cue: 250 ms following the onset of the instructing cue; 4) Pre-presentation: 500 ms preceding the opening of the box door; 5) Presentation: 500 ms following door opening (object presentation); 6) Set: 250 ms before the offset of the instructing cue; 7) Go/NoGo, from the offset of the instructing cue to the release of the hand starting position (Action condition) or 250 ms following the offset of the instructing cue (Inaction condition); 8) Grasping/Fixation: from 250 ms before to 250 ms after the Pulling onset (Action condition) or a time period ranging from 250 ms to 500 ms after the offset of the instructing cue (Inaction condition) Reward: 500 ms following reward delivery.

Single-neuron responses were statistically evaluated by means of a 9X2 ANOVA (Factors: Epoch, Condition, $p<0.01$) followed by Newman-Keuls post hoc tests. Since trials were randomized, changes of the baseline activity across trials were not expected, and the neurons showing a significant difference between baselines were discarded. Neurons were included in our dataset and were defined as *task related* when the 9x2 ANOVA revealed at least one of the two following effects: 1) a significant main effect of the Epoch factor ($p<0.01$), with the relative post-hoc tests showing a significant difference between the activity recorded in the Baseline epoch and in at least one of the other epochs (Condition-independent neurons); 2) a significant Interaction effect (Condition x Epoch, $p<0.01$), with the subsequent post-hoc tests showing a significant difference between at least one epoch of one condition and both its baseline and the corresponding epoch of the other condition (Condition-dependent neurons). Considering that the epochs of Pre-cue and Reward fall in the inter-trial period, when eye movements are not controlled, we decided to consider, for our analysis, the remaining six epochs plus the Baseline.

2.8 Data matrix construction for analyses at the population level

After single neuron analysis, we performed further analyses relying on the same data matrix and time periods. Since in all tasks most time intervals were variable (see above), to perform these analyses, we aligned neural activity on different task events, segmenting it in 20 ms bins, and considered specific time periods for each task, locked on these events, as follows.

Picture and Video tasks:

Baseline: 500 ms preceding fixation point onset; Presentation: a period of 500 ms (picture task) or 1400 ms (video task) following stimulus appearance.

Visuo-Motor task:

Baseline: from 750 ms to 250 ms before the onset of the instructing cue;

Cue: 500 ms following cue onset;

Presentation: 500 ms following object presentation;

Decision: 400 ms centered on the Go/NoGo signal;

Behavioral response: a 400 ms period, starting, in the Action condition, 300 ms before object holding, and in the Inaction condition, 200 ms after the NoGo signal.

2.9 Unsupervised clustering of neuronal responses

To identify functional clusters of neurons and assess their anatomical distribution, we performed an unsupervised clustering of the neuronal responses observed in the three behavioral paradigms. Starting from each data matrix, we calculated, for each 20 ms bin, the mean firing rate over trials belonging to each combination of the two conditions and three objects in the Visuo-Motor task, or to the same type of stimulus in the Picture or Video Task. The mean firing rate of the baseline period was then subtracted from the firing rate of each bin, obtaining the final matrices on which the cluster analyses were performed. We then applied a non-linear dimensionality reduction method, UMAP (McInnes et al., 2018), to obtain a simplified representation of these matrices. Subsequently, we performed a K-means clustering on these data, using the MATLAB *evalclusters* function, which allowed us to subdivide the considered neurons into different clusters.

The optimal number of clusters was selected by using the “cluster silhouette” metric, ranging from 1 to 10 possible clusters. Finally, to map the spatial distribution of the neurons, we calculated, for each recording site, the percentage of neurons belonging to each identified cluster, out of the total number of task-related neurons recorded on that site (3 groups: 1-30%, 31-60%; 61-100%). Then, we superimposed the resulting map onto the 2D anatomical reconstruction of the recorded brains. To more effectively show the spatial distribution of clusters, we outlined the regions hosting at least two adjacent sites. Isolated sites were considered only if containing at least 31% of neurons belonging to the cluster.

2.10 Time course of mean population activity

To characterize the time course and the discharge rate of the considered neuronal populations with respect to the main tasks phases, the neuronal activity of each population was aligned with the main behavioral events. The population activity was computed as follows. The mean single neuron activity over trials, in terms of firing rate, was calculated for each 20 ms bin in the two conditions. The average baseline activity was then subtracted from the mean single neuron activity over trials for each bin. Thus, in this analysis, 0 represents baseline activity. No normalization on the maximal firing rate was performed. Each neuron contributed one entry to each data set.

2.11 Demixed principal component analysis

In order to evaluate how the population of neurons recorded in each area encodes specific factors during the unfolding of the three tasks, we adopted a data-simplification method: the demixed principal component analysis (dPCA), using freely available code provided by Kobak and coworkers ((Kobak et al., 2016) see also (Rozzi et al., 2023)).

We performed this analysis starting, for each task, from the data matrix described above, and considering the factor ‘Type of Stimulus’ for the Picture and Video tasks (including the 12 stimuli and 6 videos, respectively), and the factors ‘Condition’ (Action and Inaction) and ‘Object’ (Cube, Cylinder and Sphere) for the Visuo-Motor task. This analysis allowed us to extract demixed principal components that captured task-related variance, either specific to the individual factors or

shared across them (Factor-independent). Specifically, we considered the demixed principal components explaining the largest proportions of *Condition*, *Object*, and *Factor-Independent* variance in the Visuo-Motor task, and of *Type of Stimulus* and *Factor-Independent* variance in the Picture and Video tasks. We used the selected components to define low-dimensional subspaces that isolate the neural dynamics associated with each experimental factor These dynamics were represented as trajectories obtained by projecting the baseline-corrected mean population activity onto the corresponding subspaces (see (Mante et al., 2013) for a similar approach).

2.12 Decoding analysis

In order to evaluate the temporal evolution of information coding by the different neuronal populations recorded in the Visuo-Motor task and if this information is encoded in static or dynamic patterns of activity, we adopted a population decoding approach according to the methodology described by Meyers and coworkers (Ceccarelli et al., 2023; Meyers, 2013). Decoding analysis was performed as described in (Rozzi et al., 2023), using the data matrix described above. In particular, for each neuron, trial-by-trial average firing rates were computed in 60 ms bins, sampled every 20 ms. Each obtained data point was then labeled according to the decoding factor of interest (Condition or Object). Data points were then randomly grouped into *k* non-overlapping splits, where *k* matched the number of data points per class (30 for Condition decoding, 20 for Object decoding). Each split included a pseudopopulation of neurons i.e., neurons recorded separately but treated as if recorded simultaneously. Next, a Poisson naïve Bayes classifier was trained on *k–1* splits and tested on the held-out split, in a *k*-fold cross-validation scheme. Finally, this entire procedure was repeated 50 times with different random splits, and decoding accuracy was averaged across repetitions to improve robustness. Note that, with respect to the results of cross-temporal decoding, our definition of *static patterns of coding* refers to the situations in which the accuracy of an off-diagonal bin is significantly greater than chance and does not differ statistically from the accuracy values of the respective on-diagonal bins (see the next section and (Ceccarelli et al., 2023)). The data alignment on task events and the binning procedure described above led to merge in the same bin the activity at the border between two subsequent periods of the task (bins of 60 ms, sampled at 20 ms intervals). Accordingly, in our analysis, we removed the last two bins of each task period considered in the analysis, obtaining a total number of 105 considered time bins.

Classification of static patterns

To investigate whether the observed *static patterns of coding* are statistically significant, we used a method employed in previous studies (Ceccarelli et al., 2023; Spaak et al., 2017). First, for each off-diagonal bin, we calculated the differences between its accuracy value and that of the two on-diagonal bins used for training and testing. The same procedure was repeated 1000 times using accuracies obtained after shuffling the labels, allowing us to obtain a null distribution of the differences in accuracy values between the off- and on-diagonal bins. For statistical analysis we selected the "significant" time bins, defined as those in which both differences were lower than 99.9% of the differences estimated at the corresponding time points in the null distribution. Then, we performed a cluster-based test (Maris & Oostenveld, 2007), by comparing the summed difference values of the observed-data clusters with the maximum summed cluster values of the null distribution. In particular, we identified clusters of consecutive "significant" off-diagonal time bins (n. bins > 0), and summed the differences observed in each point of the cluster. The same procedure was applied using the accuracy value matrices resulting from the 1000 shuffled decodings, each time extracting the maximum summed cluster values. The proportion (over the 1000 iterations) of times in which the maximum summed cluster values of the null distribution were lower than the values obtained in each observed-data cluster determined the p-value of the test. The bins for which this p value was below 0.001 were considered significantly static off-diagonal bins. Similar to (Ceccarelli et al., 2023), as a further restrictive criterion to classify the off-diagonal bins as significantly static, the two corresponding on-diagonal bins used for training and testing the classifier were required to be both significantly above chance level. In this case, we performed a permutation test consisting in evaluating the proportion of times in which the accuracy value observed in each on-diagonal time bin was higher than that observed in the null distribution, which determined the p-value of the test. The accuracy in an on-diagonal time bin was then considered significantly above chance if the obtained p-value was below 0.000009, corresponding to a p-value of 0.001 Bonferroni corrected for the 105 considered bins.

3. Results

In the results section we will 1) briefly describe the three behavioral paradigms employed; 2) describe the construction of anatomical maps based on architectural and connectional data; 3) show the distribution of neuronal responses with respect to anatomical subdivisions; 4) validate the anatomical map with an unbiased cluster analysis of functional properties; 5) compare the neuronal responses recorded in each area at the population level.

Concerning the behavioral paradigms, we employed two “passive” tasks aimed at assessing how VLPF neurons encode visual stimuli, in the absence of a specific request to use them, and a Visuo-Motor task investigating functions related to action organization (see Methods; (Rozzi et al., 2021, 2023; Simone et al., 2015, 2017)). In particular, in the Picture task (Fig 2A), the monkeys simply had to observe one of 12 pictures depicting faces, geometric solids, food or furniture; in the Video task (Fig 2B) they were required to observe one of 6 videos showing biological movements either goal related or not and object motion; in the Visuo-Motor task (Fig 2C), monkeys were instructed by two visual cues that they will have to either act on one of 3 presented objects (Action condition) or refrain from acting (Inaction condition). Then, when the object became visible, the monkeys had to wait for a go signal to perform the instructed response.

In order to define anatomical areas in the recorded brains, we relied on previous architectonical and connectional studies from our lab (Borra et al., 2011; Gerbella et al., 2007, 2010, 2013). In those studies, we had first defined the architectonic borders of areas 8FEF, 8r, 45A, 45B, 46v, and 12r and, subsequently, we injected neural tracers in these areas on 12 monkeys (see S1 Table); the different pattern of connections observed after each injection confirmed the architectonic borders and allowed to further subdivide areas 46v and 12r in three additional sectors. Here, we superimposed the areas and sectors identified in the above-mentioned studies onto the histological reconstructions of the two recorded brains, by warping both the architectonic maps and the locations of the various injection sites used to characterize the connectivity of each area (see Methods and —. Fig 1 D and E depict the results of this process. In the present work, we excluded from analysis the caudal oculomotor areas 8 and 45B and pooled together the rostral portions of 46v and 12r (hereafter defined as the *rostral sector*), since the position of the recording chambers allowed us to record only a small number of sites, especially in M2 (see Methods).

Within the investigated region, we recorded neural activity from 99 penetrations in M1 (Fig 2F) and 64 in M2 (Fig 2G). Note that, while the central part of the recorded region was densely and

homogeneously explored in both monkeys, area 45A was more sampled in M1. Furthermore, in M2, the sampling of the rostral sector was limited to its caudalmost part.

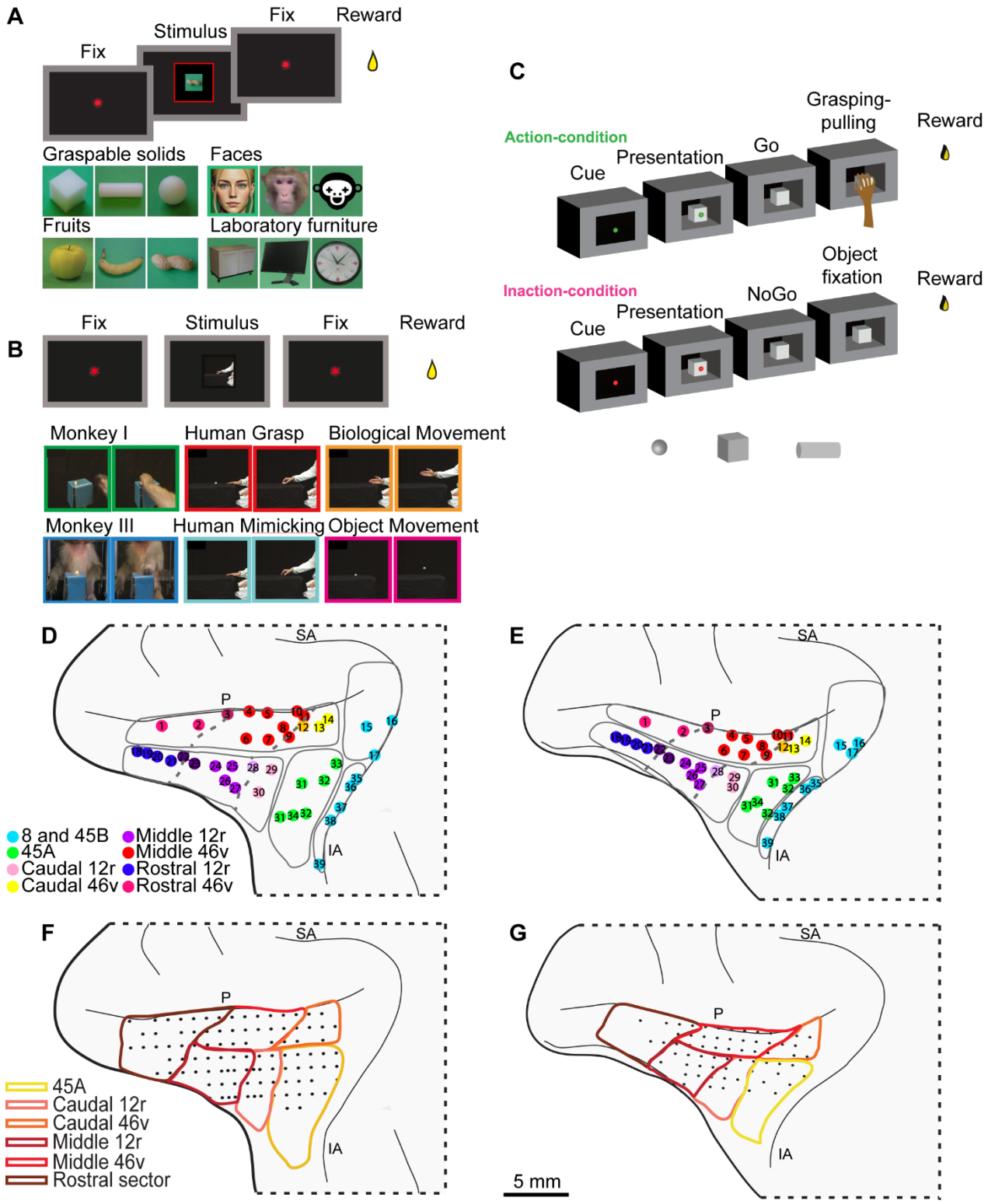

Fig 2. Behavioral paradigms and parcellation of the recorded regions. (A and B) Temporal sequence of events (above) and stimuli (below) of Picture and Video tasks. For privacy reasons, the image of the human face used in the experiment has been replaced in the figure with a

schematic representation (C) Temporal sequence of events of the Visuo-Motor task. In the bottom, the three used objects are shown. (D and E) Localization of the injection sites taken from the literature (see Methods and S1 Table), superimposed on the cytoarchitectonically defined VLPF areas of the recorded monkeys. Each dot, labelled with an index number, represents a different injection site (see S1 table for details on each labelled site). Each color refers to a specific pattern of connectivity characterizing the injection sites (Borra et al., 2011; Gerbella et al., 2007, 2010, 2013). Orange, light violet, dark violet and dark magenta dots refer to territories showing transitional connectivity. Dashed lines correspond to the borders between connectionally defined areas. (F and G) Recording grids of the two monkeys superimposed on the anatomical parcellation shown in (D) and (E). P: Principal sulcus; IA: Inferior arcuate sulcus; SA superior arcuate sulcus.

3.1 Distribution of neural responses recorded in the Picture task

We recorded a total of 2289 neurons in the Picture task , and analyzed their responses by means of a 2X12 ANOVA with factors Epoch (Baseline and Presentation) and Stimuli (the 12 presented images) ($p<0.01$, see Methods) followed by Newman-Keuls post hoc tests, which allowed us to identify neurons responding to the observation of static images and assess their possible selectivity (for the selection criteria, see Methods and (Rozzi et al., 2021)).

Neurons responding to the presentation of static images were well represented in the whole recorded region in both monkeys, except for area 45A, characterized by a lower number of responses in M1 than in M2 (Fig 3A and 3B).

Selective neurons were mostly located in caudal 46v, caudal 12r and middle 12r (Fig 3C and 3D). Fig 3E depicts the response of a caudal 46v non-selective neuron (2X12 ANOVA epoch effect $p <0.01$; interaction effect: n.s.). Fig 3F shows the response of a caudal 12r selective neuron, active only during the observation of the sphere (2X12 ANOVA interaction effect followed by Newman–Keuls post hoc test, $p < 0.01$).

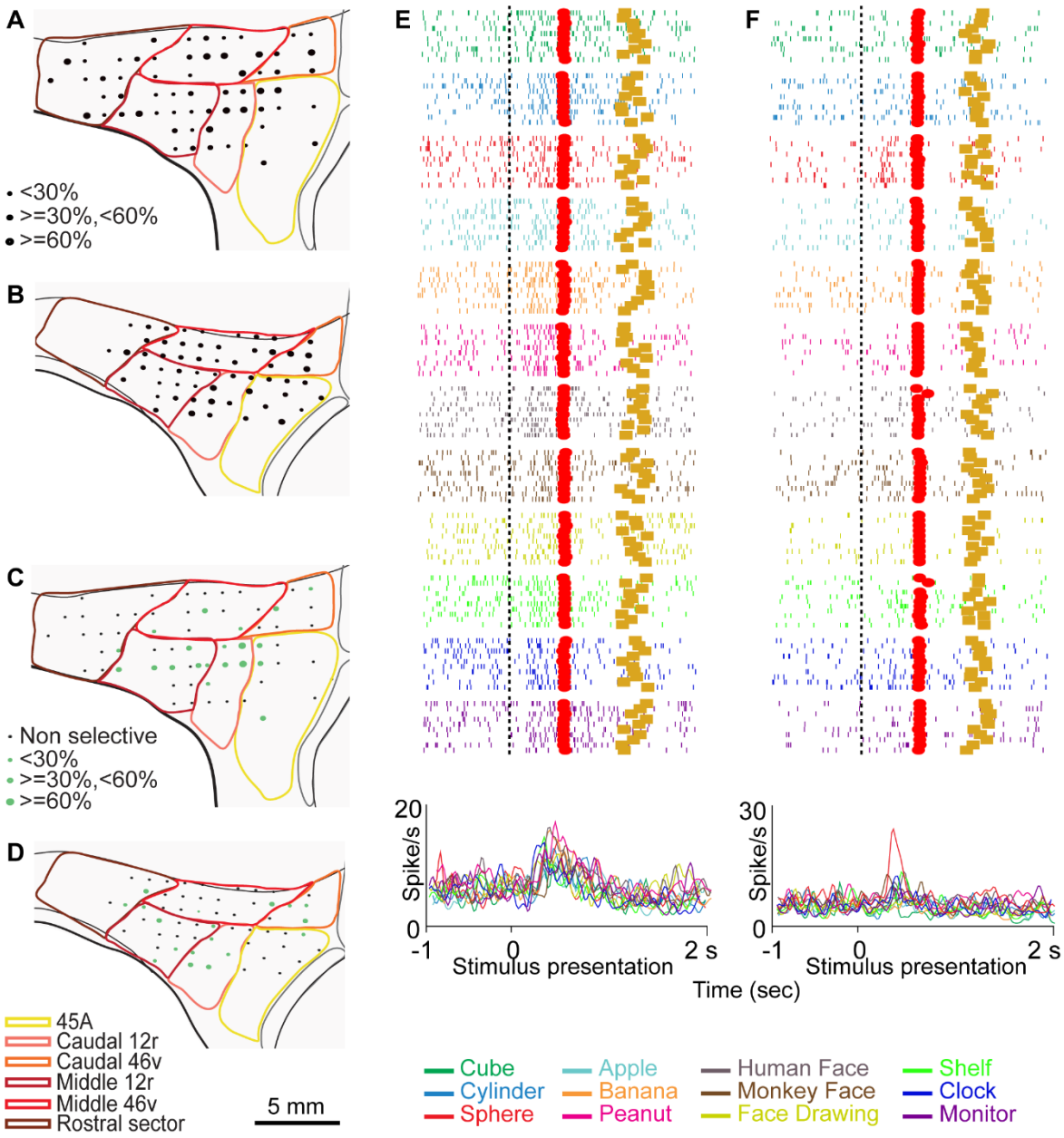

Fig 3. Distribution of functional properties in the Picture task. (A, B) Distribution of task-related neurons in the Picture task. The size of black dots represents the proportion of task-related neurons out of the total number of neurons of that site. (C, D) Distribution of selective neurons in the Picture task. The size of green dots represents, for each site, the proportion of selective neurons out of task related neurons. (E) Example of neuron showing a similar discharge profile following stimulus presentation in all conditions. (F) Example of neuron responding selectively to the presentation of the sphere. Rasters and histograms are aligned with stimulus presentation (vertical dashed line). Red squares: stimulus offset; Gold squares: reward delivery. Abscissae: time (s); Ordinates: firing rate (spikes/s).

3.2 Distribution of neural responses recorded in the Video task

We recorded a total of 2687 neurons in the Video task, and analyzed their responses by means of a 3X6 ANOVA with factors Epoch (Baseline, Video Epoch I and II) and Stimuli (the 6 presented videos) ($p<0.01$, see Methods), followed by Newman–Keuls post hoc tests, which allowed us to identify neurons responding to the observation of the videos and assess their possible selectivity according to the criteria defined in the Methods section (see also (Simone et al., 2017)).

Fig 4A and 4B show the distribution of neurons responding to the observation of videos. In both monkeys, these neurons were more concentrated in the caudal and ventral parts of the recorded region. Neurons showing a preference for at least one stimulus had a similar pattern of distribution, being mostly located in the caudal and ventral areas (Fig 4C and 4D), with a larger representation, in M2, in caudal 46v.

Fig 4E shows an example of a caudal 12r non-selective neuron responding to video presentation, independent of the observed stimulus (3X6 ANOVA epoch effect, $p < 0.01$; interaction effect: n.s.). Fig 4F depicts the activity of a caudal 12r selective neuron discharging only during the observation of a monkey grasping food, seen from a third person perspective, and exclusively in the second video epoch (3X6 ANOVA interaction effect followed by Newman–Keuls post hoc test, $p < 0.01$).

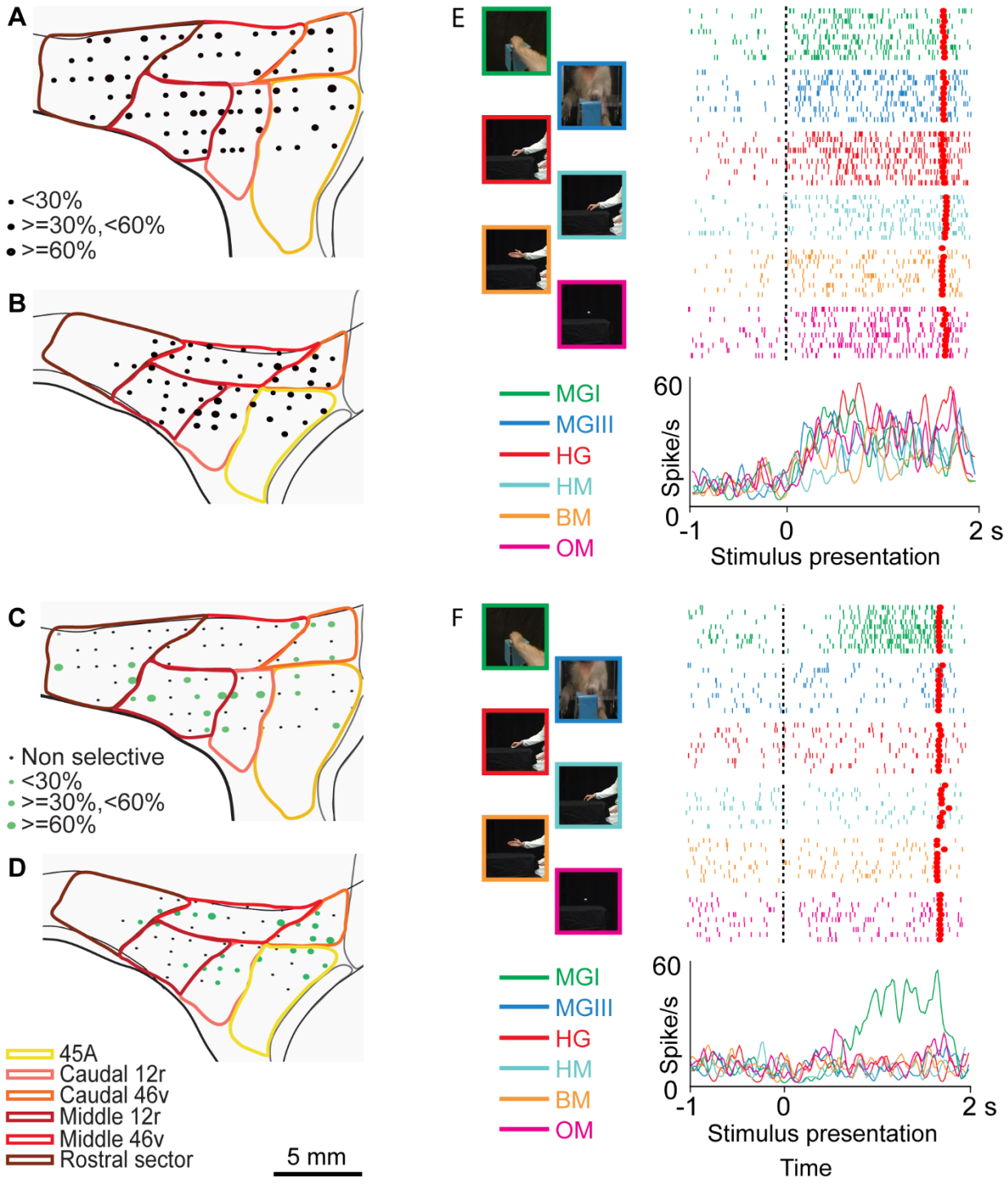

Fig 4. Distribution of functional properties in the Video task. (A, B) Distribution of task-related neurons in the Video task. (C, D) Distribution of selective neurons in the Video task. (E) Example of neuron showing a similar discharge profile following stimulus presentation in all conditions. (F) Example of neuron responding selectively to presentation of a monkey grasping in first person perspective. Other conventions as in Fig 2.

3.3 Distribution of neural responses recorded in the Visuo-Motor task

Using the Visuo-Motor task, we recorded a total of 3045 neurons. We analyzed the neuronal responses by means of a 9X2 ANOVA with factors Epoch (Baseline, Pre-Cue, Cue, Pre-Presentation, Presentation, Set, Go/NoGo, Grasping/Fixation, Reward) and Condition (Action and Inaction) ($p<0.01$, see Methods), followed by Newman-Keuls post hoc tests, which allowed us to identify task-related neurons, and assess their possible preference for one of the two task conditions in each epoch, according to the criteria defined in the Methods section (see also (Rozzi et al., 2023)). Fig 5A and 5B depict the distribution of task-related neurons in the two monkeys, that appeared to be quite homogeneously represented in the different areas.

Based on the above-mentioned statistical analysis, we identified neurons responding, in each epoch, either preferentially to one of the two conditions (Condition-dependent, see Methods) or independently of the condition (Condition-independent).

Cue-related neurons were generally well represented, in both monkeys, in the whole recorded region with a slightly lower density in middle 46v. Note that, in M1, Condition-depended neurons tended to be more represented in the central sector (middle 46v, caudal 12r and middle 12r), in M2 they were mostly distributed in the ventral part of the recorded region (area 45A, caudal 12r and middle 12r). Neurons showing a preference for the Inaction condition were much more represented than those preferring the Action condition (Fig 5C and 5D). Inaction-related neurons were less represented in caudal 46v and in the rostral sector. Fig 5E shows the discharge of a 45A Condition-dependent neuron responding to cue appearance only in the Inaction condition (9X2 ANOVA, interaction effect followed by Newman–Keuls post hoc test, $p < 0.01$).

Presentation-related responses were quite homogeneously distributed over the whole recorded region in both monkeys. However, in M1 these responses were relatively less represented in middle 12r and in 45A (Fig 5F and 5G). Condition-dependent neurons were unevenly distributed in both monkeys, being more densely represented in middle 46v, caudal 46v and middle 12r in M1 and in middle 46v, caudal 12r and middle 12r in M2. Fig 5H shows the discharge of a middle 12r Condition-dependent neuron responding to object presentation in both conditions, but significantly stronger in the Action condition (9X2 ANOVA interaction effect followed by Newman–Keuls post hoc test, $p < 0.01$).

Neurons responding during the last part of the task (*Go/NoGo-Grasping/Fixation* epoch) were well distributed, in both monkeys, along the whole explored region (Fig 5I and 5L), with Condition-dependent neurons being mainly located in its central part (caudal 12r, middle 12r, middle 46v, and caudal 46v), while area 45A and the rostral sector were mainly characterized by Condition-independent neurons. Fig 5M depicts the discharge of a middle 46v Condition-dependent neuron responding only in the Action condition (9X2 ANOVA interaction effect followed by Newman–Keuls post hoc test, $p < 0.01$). The neuron starts discharging just before the beginning of movement, peaks during object pulling, and abruptly ceases firing when the action is completed with the hand returning to the starting position.

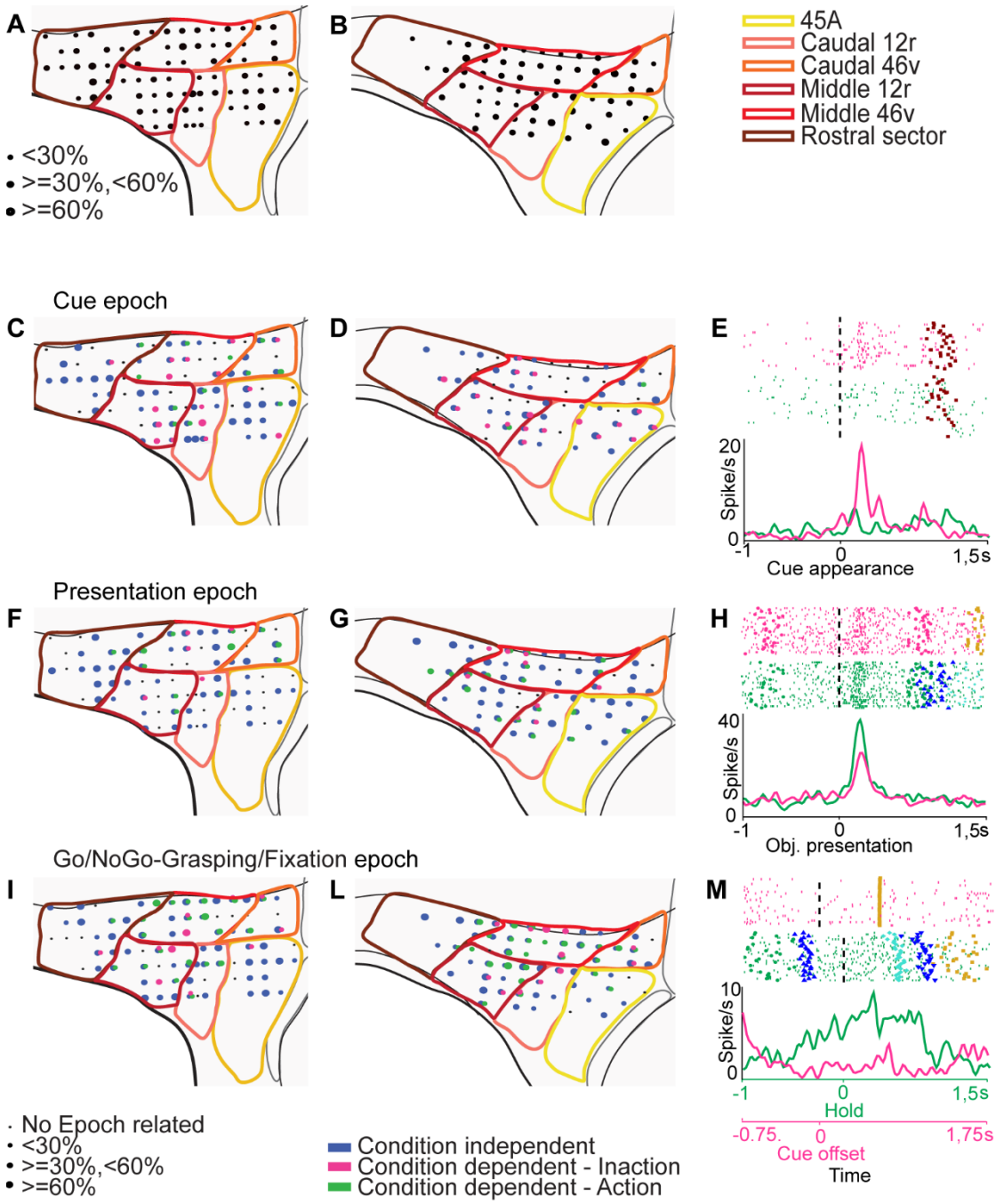

Fig 5. Distribution of functional properties neurons in the Visuo-Motor task. (A and B) Distribution of task-related neurons. (C D F, G, I, L) Distribution of Condition-dependent and Condition-Independent neurons responding during the Cue, Presentation and Go/NoGo-Grasping/Fixation epochs. Black dots represent penetration sites in which no epoch-related neurons have been recorded. Blue, green and magenta dots correspond to the sites in which Condition-independent, Action selective or Inaction selective epoch-related neurons, respectively, are represented. The size of colored dots represents the proportion of the respective category of epoch-

related neurons on the total number of task-related neurons observed in each site. (E) Example of neuron showing a preferential discharge following cue appearance in the Inaction condition. (H) Example of neuron showing a discharge rate after object presentation, which is higher during the Action compared to the Inaction condition. (M) Example of neuron showing a discharge starting from the offset of the instructing cue, only during the Action condition. Rasters and histograms are aligned (vertical dashed line) with cue onset (E), object presentation (H), and object holding/cue offset (M, for Action and Inaction conditions respectively). Green/Magenta circles: Action and Inaction cue appearance and offset, Brown squares: object presentation; Blue upward triangles: release of the hand from the starting position; Blue downward triangles: return of the hand on the starting position; Gold squares: reward delivery. Other conventions as in Fig 2.

3.4 Unsupervised clustering of task-related neurons

To verify whether the distribution of functional properties aligns with the above described anatomical parcellation, for each task, we performed an unsupervised clustering of firing rates of task-related neurons, using their representation on the UMAP embedding (see Methods). We first performed this analysis on the whole population of task-related neurons (see Methods for the selection criteria) of the Picture, Video and Visuo-Motor tasks. For each task, we identified two functional clusters. S1 Fig depicts the distribution of neurons belonging to each cluster (see Methods for details on map construction). Functional clusters were distributed along the whole recorded region, thus not showing any clear distinction between areas. S1 Fig also shows the baseline-subtracted mean firing rate for the populations of neurons in each identified cluster. For each task, these neurons showed a modulation of activity time locked to the main events of the tasks. More specifically, one cluster was typically characterized by an increase in firing rate after each event, with the strongest response following stimuli/object presentation, while the other showed a strong peak of discharge aligned with the first task event/task beginning, followed by a prolonged and general decrease of the firing rate.

The same analysis was performed on neurons classified as selective in the Picture and Video tasks and as Condition-dependent in the Cue, Presentation or Go/NoGo-Grasping/Fixation epochs of the Visuo-Motor task (see Methods for the selection criteria). Differently from the above-described distribution of task related neurons, these clusters covered smaller and more localized

regions (S2 Fig). The anatomical distribution of functional clusters related to the responses to visual stimuli in the Picture and Video tasks and to the final phases of the visuo-motor task, was very consistent in the two monkeys, while that associated to condition-dependent Cue and Presentation responses showed some difference between monkeys.

This analysis allowed us to observe that, in both monkeys, functional subdivisions overlap with anatomically defined areas, confirming each anatomical border. For example, this was evident when considering middle 46v, which was characterized by a strong representation of clusters related to the final phase of the visuo-motor task and by the almost complete absence of clusters related to selective responses in the passive tasks, instead represented in the neighbouring caudal and ventral areas. Another functional border can be observed between caudal and middle 12r, with clusters related to final phases of the visuo-motor task more consistently represented in the middle than in the caudal sector of area 12r, and clusters related to the appearance of visual stimuli (both in the passive and the visuo-motor tasks) tending to be more represented and overlapping in caudal 12r.

Clustering analysis confirmed, in both monkeys, our anatomical parcellation of the VLPF, thus allowing us to analyze and compare the population data related to the identified anatomo-functional areas, considering the two monkeys together.

3.5 Representation of task relevant factors in VLPF areas

To evaluate how the population activity of the different VLPF areas is modulated by task relevant factors, for each task we performed demixed principal component analysis (dPCA, see Methods) on task-related and on all recorded neurons. This analysis allowed us to identify those components explaining variability that is related to the factors considered in each task, as well as factor independent variability. These components were then used to define low-dimensional subspaces that isolate the neural dynamics associated with each experimental factor. The resulting dynamics are represented by the neural trajectories shown in the figures described in the following paragraphs (see (Mante et al., 2013) for a similar approach, and Methods for further details).

Picture task

Fig 6 and S3 Fig show that the trajectories of each area were characterized by peaks linked to stimulus presentation, represented by deflections along the Factor-independent axis. The

distinction between trajectories representing the different stimuli (Type of stimulus axis), is very evident only in caudal 12r.

Video task

Fig 7 and S4 Fig show that the trajectories of each area were characterized by peaks linked to video presentation, represented by deflections along the Factor-independent axis. The distinction between trajectories representing the different videos (Type of stimulus axis), is very evident in caudal areas (45a, caudal 12r and caudal 46v) and in middle 12r. Note that in caudal 12r and caudal 46v, the trajectories representing stimuli belonging to similar categories (Simone et al., 2017) are grouped together.

Visuo-motor task

Fig 8 and S5 Fig show that the trajectories of each area are characterized by peaks linked to the main task events (e.g. cue onset, object presentation, cue offset), represented by deflections along the Factor-independent axis. In each area, trajectories were clearly separated on the Condition axis (Action and Inaction). However, this separation is less evident in 45A and the rostral sector. Concerning the other areas, this segregation occurred just after cue appearance in caudal 46v and middle 12r, and later, between cue and object presentation, in middle 46v, whereas this separation occurred only after object presentation in caudal 12r. Moreover, trajectories maintained their separation after the cue offset in middle 12r and middle 46v, while in caudal 12r and caudal 46v, in this period, they converged toward their origin.

Concerning the Object axis (Cube, Cylinder and Sphere), all areas except 45A and rostral sector showed a separation of the trajectories after object presentation. Interestingly, object-related separation was apparently more evident in the Action than in the Inaction condition.

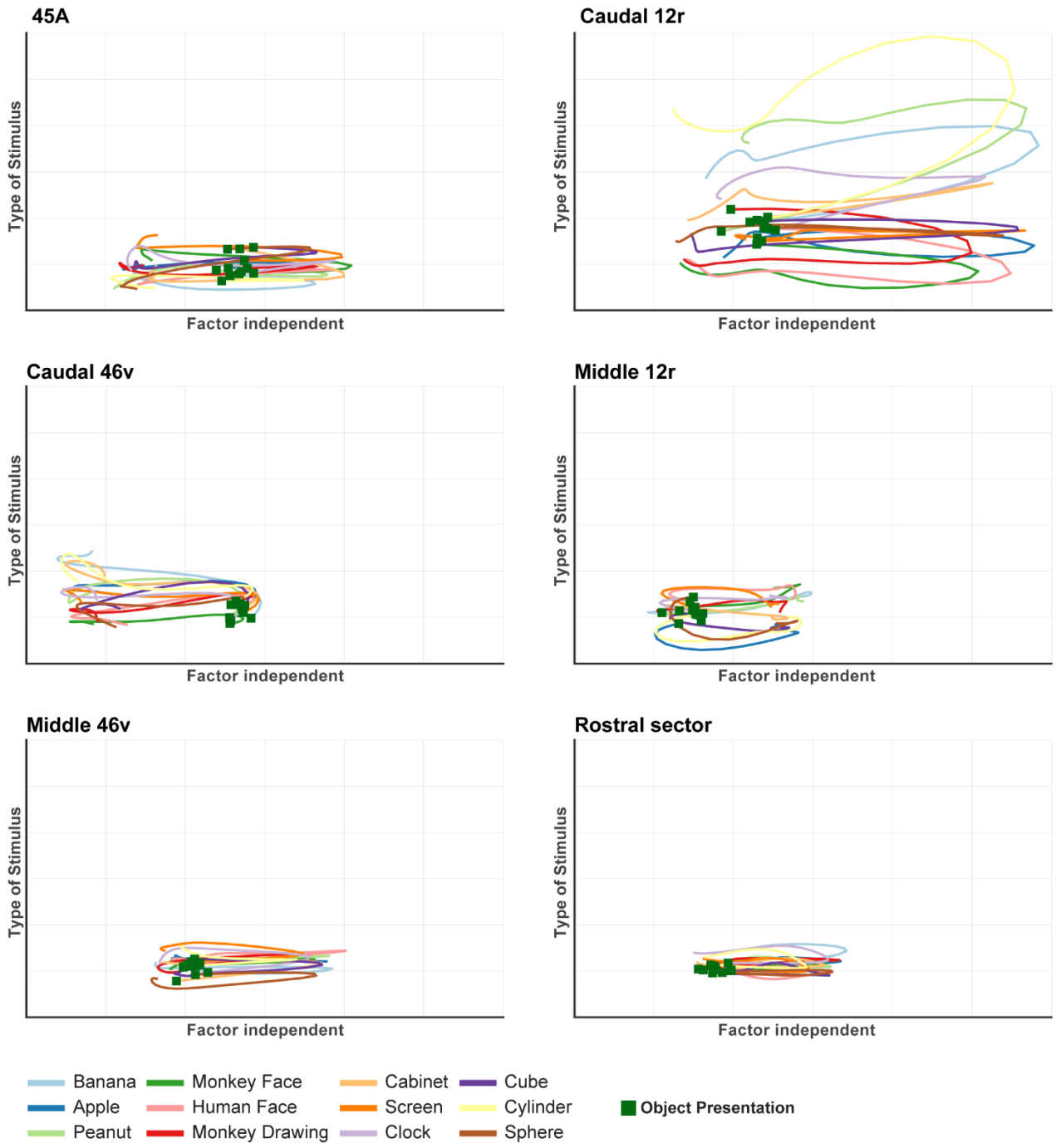

Fig 6. dPCA trajectories of each VLPF area in the Picture task. Each panel depicts the time course of the first Factor-Independent (X axis) and of the first Type of Stimulus-related (Y axis) principal components plotted together, relative to the population of task-related neurons recorded in each area. Each colored line corresponds to one of the twelve stimuli presented in the task. Green squares represent the time at which the stimulus presentation occurs.

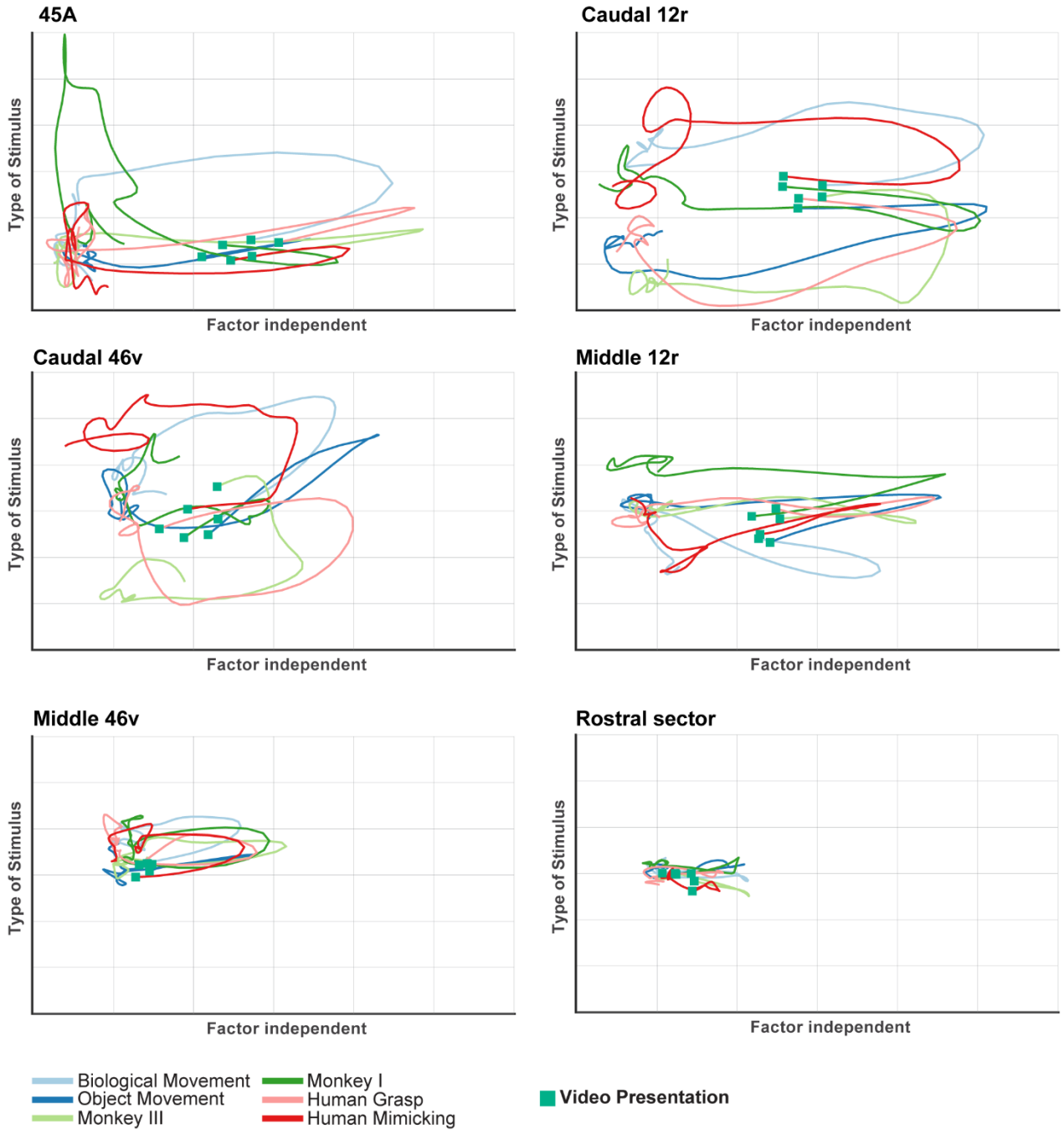

Fig 7. dPCA trajectories of each VLPF area in the Video task. Each panel depicts the time course of the first Factor-Independent (X axis) and of the first Type of Stimulus-related (Y axis) principal components plotted together, relative to the population of task-related neurons recorded in each area. Each colored line corresponds to one of the six videos presented in the task. Green squares represent the time at which the stimulus presentation occurs.

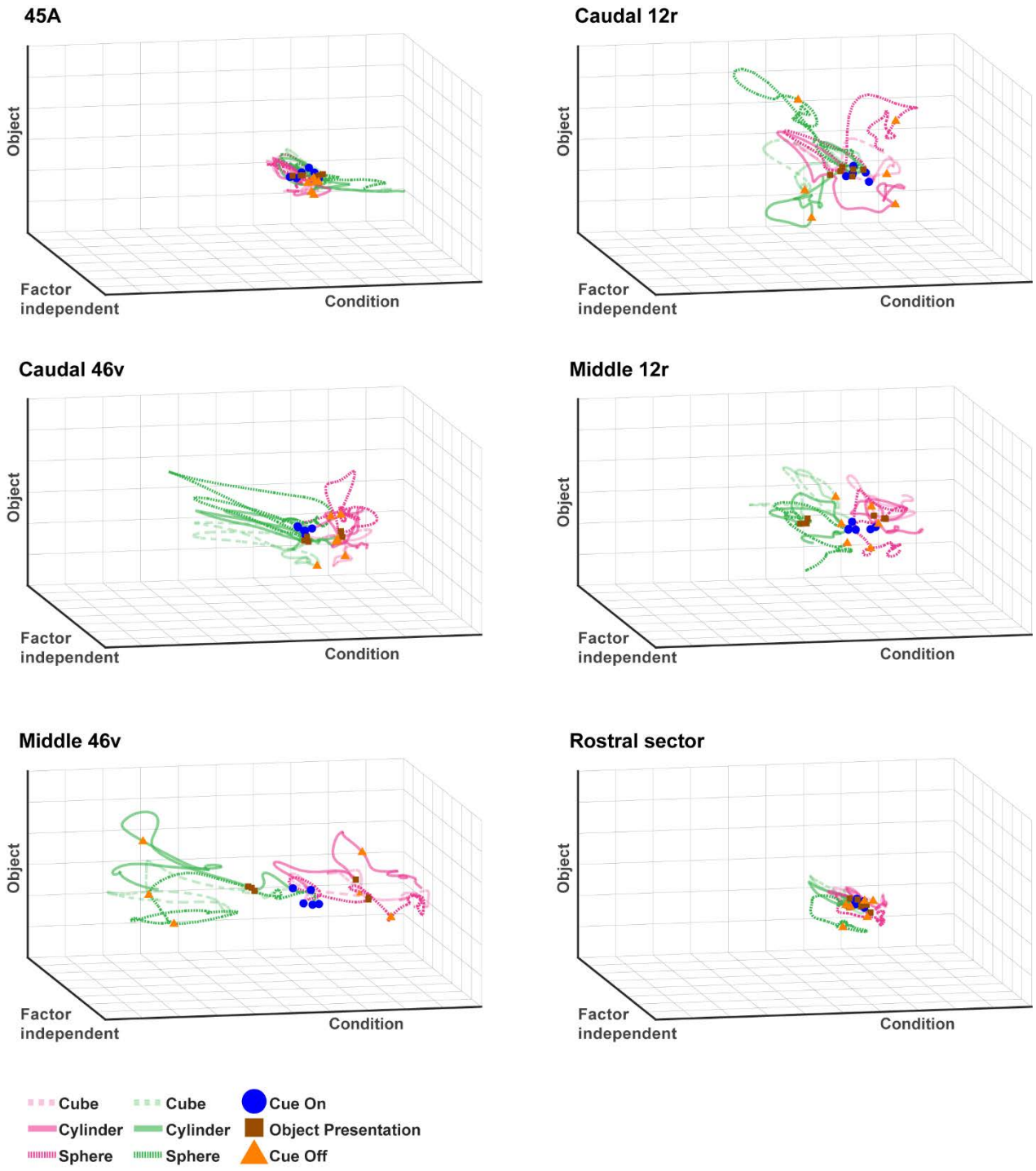

Fig 8. dPCA trajectories of each VLPF area in the Visuo-Motor task. Each panel depicts the time course of the first Condition-related (X axis), of the first Object-related (Y axis) and of the first Factor-Independent (Z axis) principal components, relative to the population of task-related neurons recorded in each area. Green and Magenta colored lines represent Action-related and Inaction-related trajectories, respectively. Continuous and dashed lines correspond to the three objects presented, respectively. Blue circles, brown squares, and orange triangles represent, for each trajectory, the time of cue onset, object presentation, and cue offset, respectively.

3.6 Population activity of VLPF areas in the Visuo-Motor task

In order to evaluate the response of the population of neurons recorded in the different VLPF areas, we plotted, for each of them, the baseline-subtracted activity (see Methods) of task-related neurons (Fig 9) and of all recorded neurons (S6 Fig) in the Action and Inaction conditions.

Both analyses showed that all areas share, as a common feature, the presence of two clear peaks following cue and object appearance. The peak related to cue presentation during the Inaction condition was higher than the one observed during the Action condition in all areas, except for caudal 46v, where this pattern is inverted. The object presentation-related peak was, in all areas, higher than the cue-related one, with the Action condition always eliciting a stronger neural population activity than the Inaction one during this period.

The pattern of responses observed in the final part of the task (starting around the Go/NoGo signal) was quite heterogeneous when comparing the different areas (Fig 9 and S6 Fig). Some areas were primarily characterized by an enhanced population response, while others displayed a suppressed response (i.e., below baseline level). In particular, the rostral sector exhibited suppressed population activity in both Action and Inaction conditions, while 45A showed activity suppression only in the Inaction condition. Caudal 46v demonstrated slight suppression of activity, mainly occurring in the Action condition just before the Go/NoGo signal. Note that when considering the population of task-related neurons (Fig 9), the activity suppression observed in this condition is also maintained during object holding. Caudal 12r population activity began to increase in both conditions following the Go/NoGo signal, reaching a peak after about 250 ms. In the Inaction condition, the activity remained sustained until reward delivery, then sharply falling below baseline level. In contrast, in the Action condition, sustained activity ended with the beginning of holding, abruptly dropping to baseline level during this period, and decreasing below it after reward delivery. Middle 12r was characterized by a sustained increase in firing rate only during the Action condition. The population response began to grow after the Go signal, reaching a peak around the start of the holding. Then, the activity decreased to baseline level, while the monkeys continued pulling the object. In both conditions, there was a final lower peak after reward delivery. Middle 46v exhibited the highest mean-net activity among all the areas considered in the final task segment of the Action condition. Notably, while no clear enhancement or suppression was evident in the Inaction condition, in the Action condition the activity increased after the Go signal, continued to rise during reaching and grasping execution, peaked around the start of holding, and gradually decreased while the monkeys held the object, returning to baseline level around reward delivery.

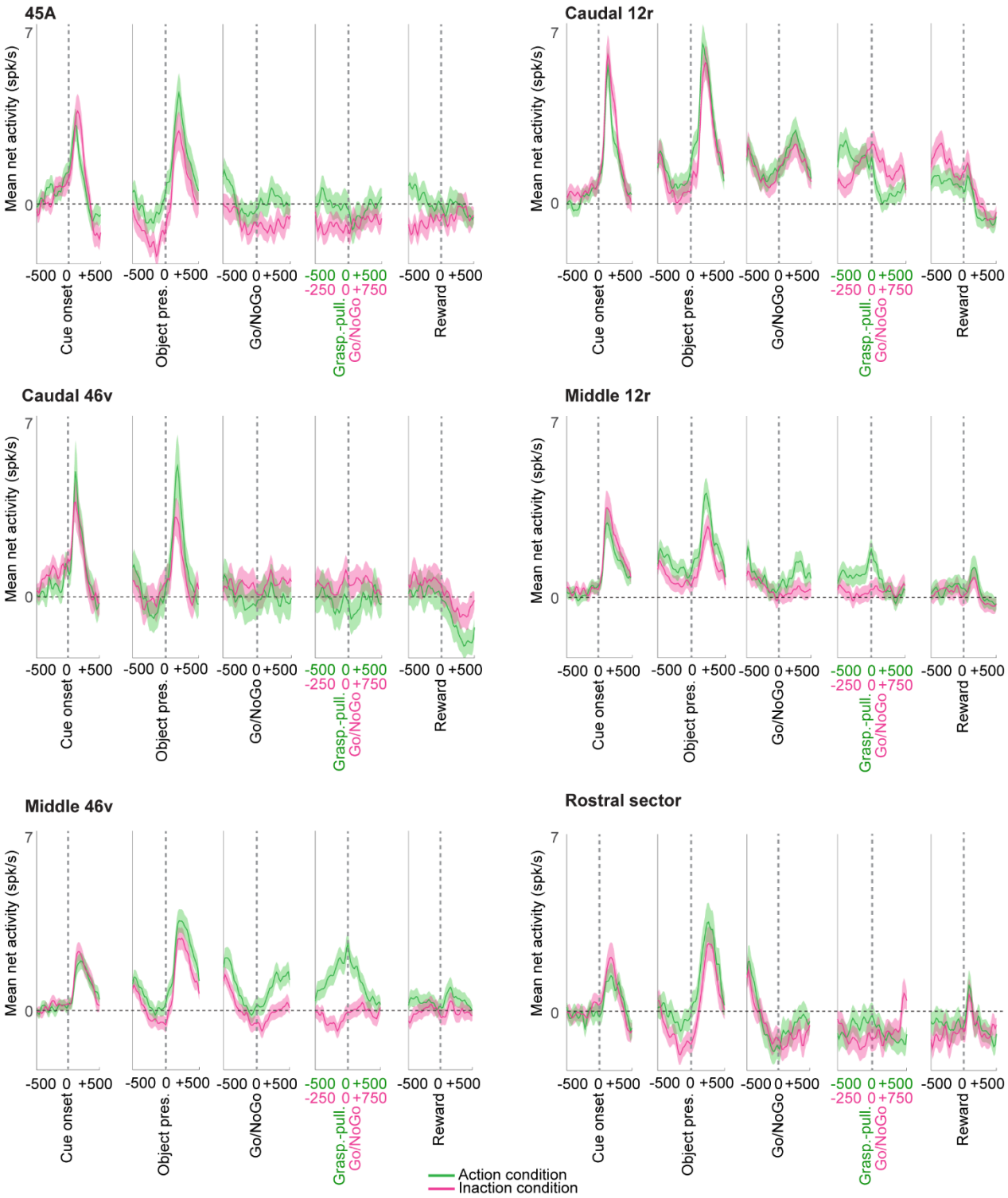

Fig 9. Mean population activity of neurons recorded in each area during the Visuo-Motor task. Temporal profile of mean net activity of the population of task-related neurons recorded in each of the considered VLPF areas. The magenta and green curves indicate the population mean net activity in the Inaction and Action conditions, respectively. The shaded area around each curve represents standard errors. The dashed line indicates baseline-level activity. The neuronal activity is aligned on the main task events indicated below each panel of the figure.

3.7 Decoding of the condition and object factors in VLPF areas

We adopted a cross-temporal decoding analysis on the neural activity recorded in the Visuo-Motor task to assess, in a time-detailed manner, which type of information was encoded by the studied areas. In particular, this approach consisted in training a classifier in decoding the Condition or Object on a specific time point and testing it on the same or on all others (see Methods for details). This allowed us to assess whether a high and significant level of accuracy was achieved not only when training and testing the classifier on the same time bin (on-diagonal time points), but also when the training and testing phases involved different periods (off-diagonal time points; see Methods for details). We refer to the latter case as a 'static pattern' of coding, indicating that a similar neural code, associated to the analyzed factor (Condition or Object) is maintained across the training and testing periods.

Fig 10 and S7 Fig show the accuracy level of the decoding of the Condition (A-F) and the Object (A'-F') factors observed in both on and off-diagonal time points (see Methods). Similarly to what was described above, we observed, for each area, strong consistency between the results based on task-related and the whole population of recorded neurons, thus we will describe them together (Fig 10 and S7 Fig).

The Cross-temporal decoding analysis showed that some functional features are shared by all the investigated areas, while others characterize each of them. Considering the Condition factor, in each area, a very high and significant level of accuracy was evident on the diagonal, when the classifier was trained and tested on the same time bins (permutation test $p<9.5e-6$, Bonferroni corrected for the number of on-diagonal time bins, see Methods), with a relative decrease in accuracy typically occurring around the Decision period.

Besides the important similarities among areas, which are evident when considering the accuracy levels along the diagonal, static patterns involving different task periods characterized each area. In area 45A, a static pattern of coding was observed between the final phase of the Cue period and the final part of the Behavioral response period (cluster-based permutation test, $p<0.001$, see Fig 10, S7 Fig and Methods). Note that this pattern was "bi-directional", being present both when training on the Cue period and testing on the Behavioral response one and *vice versa*. In caudal 12r, a static pattern of activity was observed among the Presentation, Decision and Behavioral response periods (cluster-based permutation test, $p<0.001$; Fig 10 and S7 Fig), being

equally evident in both decoding “directions”. A static pattern of coding was instead observed, in caudal 46v, across various time periods: Cue, Presentation, and a phase extending from the end of the Decision period to the beginning of Behavioral response one (cluster-based permutation test, $p<0.001$; Fig 10 and S7 Fig). Note that the static pattern observed in this area was not clearly “bi-directional”, being mostly evident when training the classifier on the last part of the task and testing it on the Cue and Presentation periods. Considering middle 12r, cross-temporal decoding of the Condition factor revealed that a high and significant level of accuracy was present when training the algorithm on the Decision period and testing it on the Cue and Behavioral response period (cluster-based permutation test, $p<0.001$; Fig 10 and S7 Fig). In middle 46v, a very consistent and “bi-directional” static pattern of coding occurred during an extended period of the task, encompassing the Presentation, Decision and Behavioral response periods (cluster-based permutation test, $p<0.001$; Fig 10 and S7 Fig). Finally, in the rostral sector, a static pattern of coding, though associated with a quite low level of accuracy, was observed only when training the classifier on the Decision period and testing it on the Behavioral response one, and vice versa (cluster-based permutation test, $p<0.001$; Fig 10 and S7 Fig).

Taking into account the Object factor, a very high and significant accuracy was always observed, in each area, along the diagonal during the Presentation period (permutation test $p<9.5e-6$, Bonferroni corrected for the number of on-diagonal time bins, see Methods). Note that this effect was mostly limited to this period in areas 45A, middle 46v and in the rostral sector (Fig 10 and S7 Fig), while caudal 46v, caudal 12r and middle 12r consistently showed very high and significant levels of accuracy, along the diagonal, from the Presentation period onwards. In addition, these latter areas were also characterized by a “bi-directional” static pattern of coding that was observed from the final phase of the Presentation period onwards (cluster-based permutation test, $p<0.001$), and that was especially evident in caudal 12r.

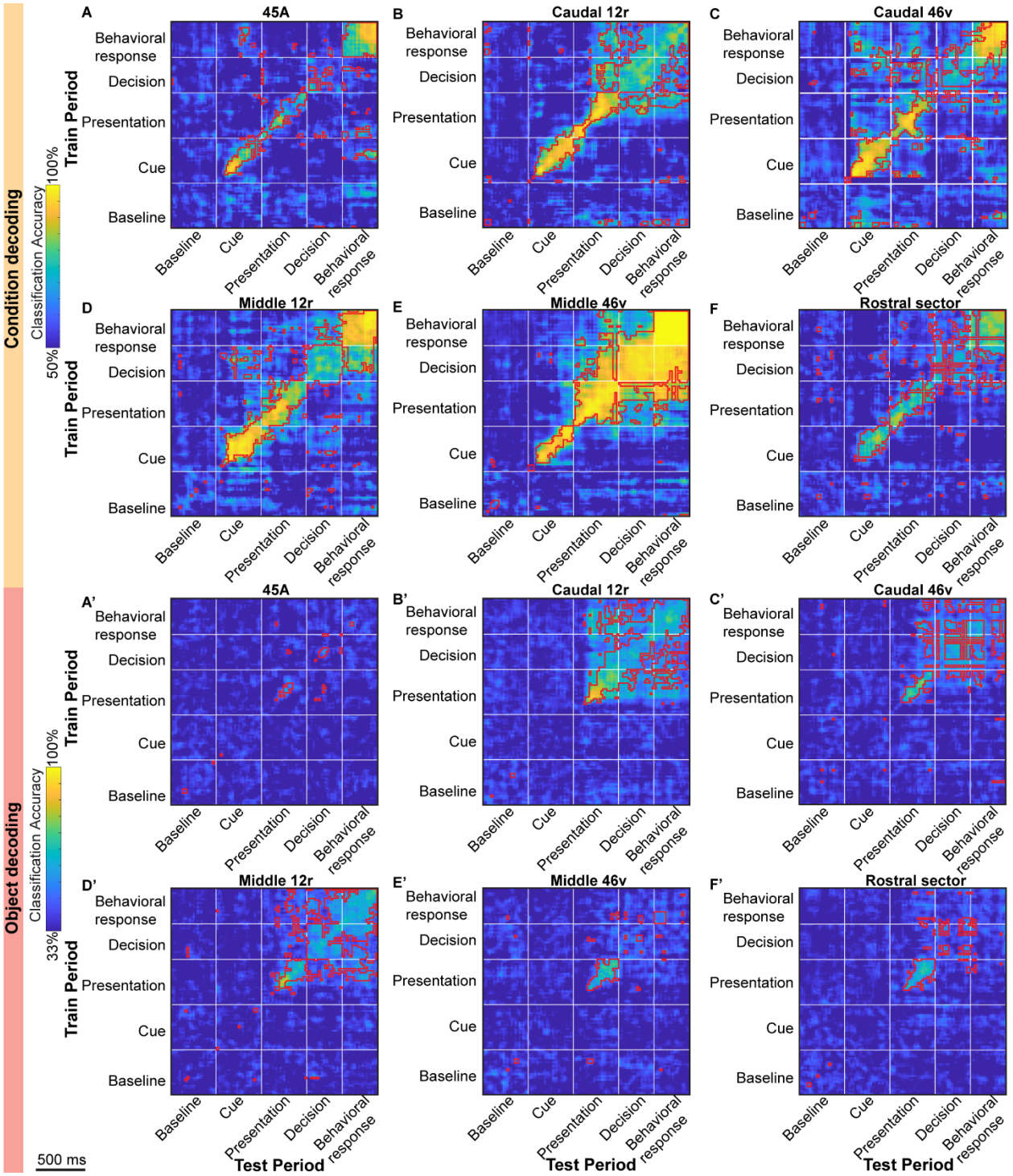

Fig 10. Cross-temporal decoding of the Condition (A-F) and Object (A'-F') factors of the Visuo-Motor task in task-related neurons. For each analysis, the decoding accuracy is computed in bins of 60 ms, sampled at 20 ms intervals. For each plot, the white vertical and horizontal lines delimit the considered time periods (see Methods). Decoding periods of testing and training are indicated on the X and Y axes, respectively. For each plot, red outlines delimit statistically significant time bins (on and off-diagonal, see Methods).

4. Discussion

In the present study, we investigated the specific contribution of different VLPF areas in processing sensory information and exploiting it for guiding behavior. To this aim, we recorded neuronal activity from a large sector of monkey VLPF, covering about its posterior two-thirds, during tasks involving either the passive processing of visual stimuli or their use for guiding reaching-grasping actions.

Under the hypothesis that the connectional features of different areas underpin functional specificity, we adopted an anatomical parcellation produced by our group (Borra et al., 2011; Gerbella et al., 2007, 2010, 2013) and validated it on a functional ground by using an unsupervised clustering analysis. Then, we analyzed the neuronal activity of each identified anatomical area showing that some functional features are broadly distributed, while others characterize each area.

Our main results show that:

- The coding of different task phases and the behavioral rule is observed across all recorded areas, indicating a distributed representation of these processes within VLPF, which is in line with the strong interconnection among prefrontal areas (Borra et al., 2011; Gerbella et al., 2013);
- The passive presentation of visual stimuli primarily activates neurons in the caudal VLPF areas, especially in caudal 12r. This suggests that these areas, consistently with their strong connections with the inferotemporal cortex (Borra et al., 2011), represent the first VLPF stage of visual processing;
- The actual execution or withholding of grasping actions predominantly activates neurons in the intermediate VLPF areas, particularly in middle 46v. This indicates that these areas, in line with their strong connections with the parietal and premotor cortices (Gerbella et al., 2013), may primarily contribute to action selection and guidance;
- Each area differently contributes to the encoding of visual features and to the exploitation of contextual information for guiding behavior.

A summary view of our findings is shown in Fig. 11.

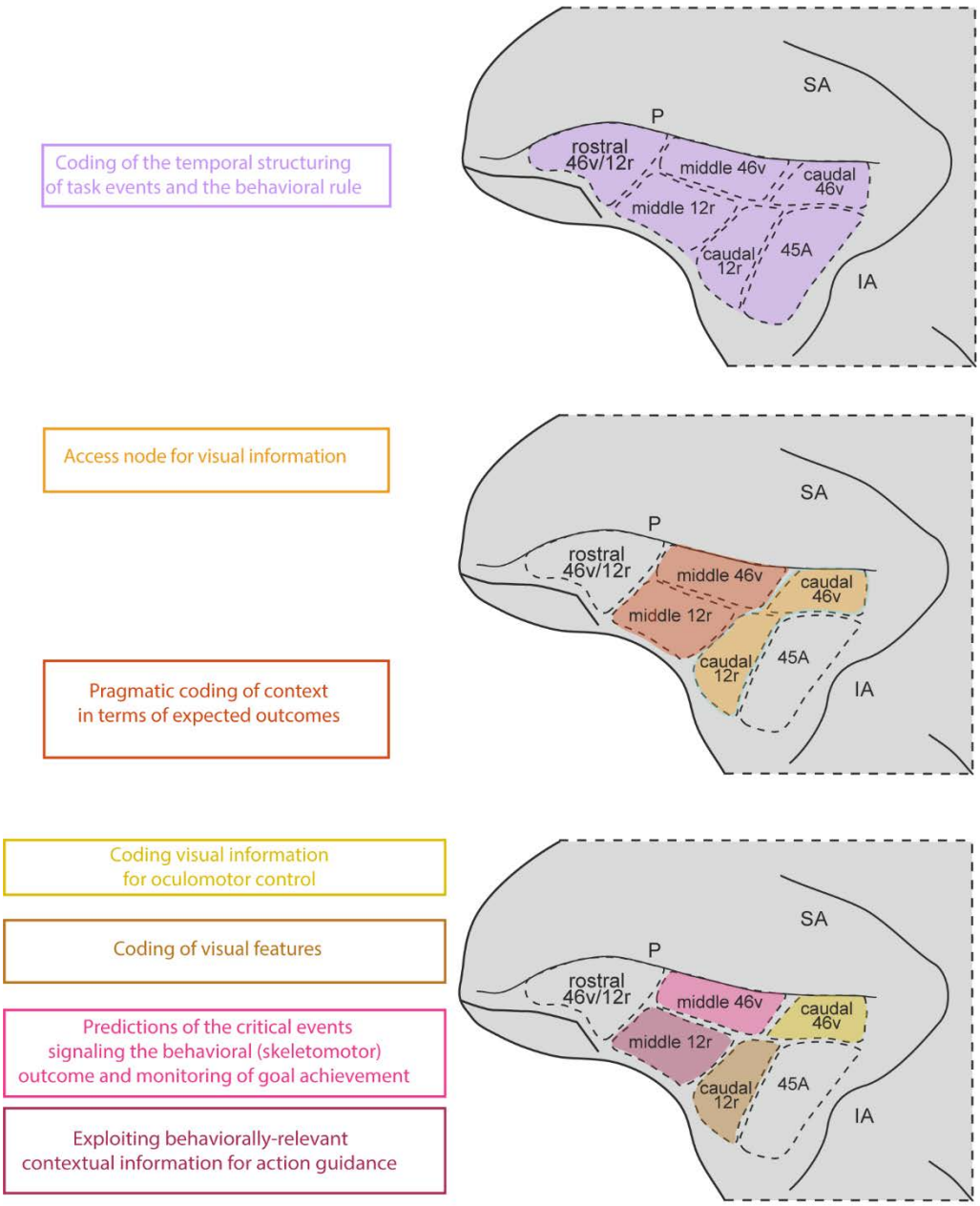

Fig 11. Overview of the distribution of functional properties in VLPF.

P, Principal sulcus; IA, inferior arcuate sulcus; SA, superior arcuate sulcus.

4.1 Comparison with previous mapping studies

In the past, several studies tried to functionally subdivide LPF by using visual stimuli either passively presented or in a context of working memory tasks (Markowitz et al., 2015; Ó Scalaidhe et al., 1997; Riley et al., 2017; Tan et al., 2023); however, these tasks were usually examined in isolation from one another. An exception is represented by the work of Tanila and colleagues, who studied neural activity in a large peri-principal region during the presentation of visual, auditory, and somatosensory stimuli, as well as during the execution of hand and eye movements in a naturalistic context (Tanila et al., 1993). Interestingly, they found that visual responses were most densely represented in caudal VLPF, where also oculomotor neurons have been recorded, and somatic responses (i.e. those to somatosensory stimulation and/or associated to the execution of reaching-grasping actions) were primarily found in intermediate VLPF. Accordingly, they suggested the presence of a functional distinction among different prefrontal sectors, based on their connectional properties. Indeed, they matched the distribution of single neurons characterized by specific functional properties with an anatomical framework based on connectional studies in which large injections, encompassing more than one cytoarchitectonic area, were performed (Cavada & Goldman-Rakic, 1989a, 1989b; Chavis & Pandya, 1976; Neal et al., 1990; Petrides & Pandya, 1984; Seltzer & Pandya, 1989). Similarly, in our study, we started from the hypothesis that each anatomical area is characterized by specific functions depending on its pattern of connections. However, differently from Tanila and coworkers, we employed as a reference framework a more refined multi-architectonic and connectional parcellation from our group, then we functionally validated it using an unsupervised clustering approach and, finally, used this parcellation to verify whether different areas have different functions. Another difference with Tanila's study is that, in order to study single neurons responses, we used well controlled paradigms. Thus, our study on the one hand confirms the pioneering observations of Tanila and coworkers, on the other, identifies the specific functional role in visual processing and context-based behavioral organization of the different VLPF areas.

More recently, a mapping of visual responses in LPF has been described in a series of studies performed by the group of Constantinidis (Riley et al., 2017, 2018; Trepka et al., 2024). Although it is difficult to directly compare our data with their findings, mainly due to the use of markedly different anatomical frameworks, some clear similarities can be found. Indeed, in a recent study (Riley et al., 2018), the authors compared the responses to passive presentation of visual stimuli with those elicited by the same stimuli when used in a working memory task. They demonstrated

that: posterior regions are typically more involved than anterior ones in coding visual stimuli during stimulus presentation and delay phases of the tasks, independently of whether the task was passive or memory related, while anterior areas are typically more involved in the memory task than in the passive one (Riley et al., 2018). In other words, these authors described the presence of a rostro-caudal functional gradient within the prefrontal cortex, in which posterior areas are more involved in coding visual information per se, while more anterior regions have a stronger role in exploiting visual information to guide behavior. Our results generally confirmed this type of functional organization, allowed us to extend this idea from working memory to action organization and showed that each area gives a partly different contribution within this gradient.

4.2 Coding of task phases and behavioral rules is broadly distributed in VLPF

Single neuron analyses reveal that task-related neurons recorded in the different behavioral paradigms are broadly represented along the whole investigated VLPF region (Figs 3-5 A, B). Considering the results of the analyses at the population level, it emerges that all areas show multiple peaks of activity related to the main task events, indicating that they are all involved in coding their temporal structuring (Figs 8 and 9, S1 Fig). Another shared function corresponds to the coding of the behavioral rule as shown by the decoding and principal component analyses on the Visuo-motor task (Figs 8 and 10). Altogether, these results are in line with a large body of literature on the functional role of prefrontal neurons (Miller & Cohen, 2001; Saga et al., 2011; Tanji & Hoshi, 2008; Wallis et al., 2001; White & Wise, 1999).

Note that our data fit well theoretical models describing the adaptability of functional properties in the prefrontal cortex (Assem et al., 2020; Duncan, 2001, 2010; Kadohisa et al., 2023), which propose that, although neurons encoding different types of information are broadly distributed, different subregions are characterized by a maximal sensitivity to a specific type of information. These models also propose that the complexity of the paradigms and the level of analysis might influence the possibility to describe a broader distribution of properties or the presence of regional specialization. Our task design, and the employed analyses allowed us to demonstrate that specific and distributed functions coexist in VLPF.

4.3 The posterior region of VLPF constitutes an access node for visual information

The data from our visual tasks show that caudal and ventral VLPF areas are strongly involved in processing passively presented visual stimuli, independently of any association with a behavioral outcome. More specifically, our results show that selective responses to passive stimuli are strongly represented in caudal 12r, caudal 46v, and, to a lesser extent, middle 12r. This is also reflected by the dPCA showing, in these areas, a clear separation of the trajectories relative to the different stimuli. Interestingly, when considering the Video task, trajectories relative to stimuli belonging to the same semantic category (Simone et al., 2017) appear to be grouped together within these areas. These functional properties strongly resemble those described by previous electrophysiological studies on caudal prefrontal areas (Ó Scalaidhe et al., 1997; Riley et al., 2018; Trepka et al., 2024; Wilson et al., 1993) and high order temporal visual areas (Logothetis & Sheinberg, 1996; Tanaka, 1996) and are in line with the fact that caudal 12r, caudal 46v, and middle 12r show strong connections with temporal visual areas (Borra et al., 2011; Gerbella et al., 2007, 2013). Thus, we propose that these prefrontal areas represent the first stage of processing of the visual input reaching VLPF. Considering the Visuo-Motor task, in line with the data obtained in the passive tasks, decoding analyses show that caudal areas 46v and 12r and, to a lesser extent, middle 12r present a clear pattern of object coding which is shared between the phases of the task going from object presentation onward, indicating that caudal and ventral VLPF areas are more strongly involved in coding object-related visual information also when the stimuli are actively used to guide the behavior.

Among caudal areas, 45A appears less involved in visual processing. Indeed, in this area we recorded a smaller number of responses to passively observed visual stimuli than in caudal 12r and caudal 46v. Noteworthy, this area has strong connections with posterior temporal areas providing visual and auditory information, including communicative stimuli, and with prefrontal regions and subcortical structures involved in oculomotor control and gaze orientation (Borra et al., 2015; Borra & Luppino, 2021; Gerbella et al., 2010). Thus, it is possible that the lower number of visual responses in this area with respect to the other caudal VLPF regions is due to the fact that its neurons typically respond to acoustic stimuli or to visual-acoustic stimuli combination (Romanski, 2007; Romanski & Sharma, 2023), which were not included in our paradigms.

4.4 The intermediate region of VLPF exploits visual information for guiding actions

Our Visuo-Motor task allowed us to observe that the middle part of the investigated region is deeply involved in exploiting visual information for action guidance. Considering Condition coding in the Visuo-Motor task, middle 46v and, to a lesser extent, middle 12r and caudal 46v, are characterized by the strongest Condition-related differentiation (dPCA) and, as observed with the decoding analysis, by a very high accuracy in discriminating between conditions, with a stable coding observed across the initial and final phases of the task (see below). It is worth noting that in the Visuo-Motor task the monkeys can already decide whether to act or withhold actions during the Cue period, based on cue color (green or red, respectively), but the decision on the specific motor program to employ in the Action condition can only occur after object presentation. Thus, the static pattern observed between the initial and final phases of the task could partly reflect the structure of our task.

In addition, neurons showing a preference for the Action condition during object presentation are well represented in middle areas 46v and 12r, with some differences among monkeys. This evidence is in line with the functional gradients observed in literature (Riley et al., 2018; Trepka et al., 2024), showing that these prefrontal regions have a stronger involvement in coding visual stimuli when these latter are actively exploited in relation to a subsequent behavioral response. Noteworthy, these areas are also characterized by the strongest representation of neurons showing a preference for the Action condition in the final phases of the task, hence during action programming and execution, in line with their strong connections with the parieto-premotor nodes of the grasping circuit (Borra et al., 2011, 2017; Gerbella et al., 2013).

Overall, these results indicate that the intermediate/dorsal areas of VLPF are strongly involved in encoding the behavior associated to the actual context.

4.5 VLPF areas show partially different contributions to action organization

Within the above described general trend, we were also able to observe some peculiarities characterizing each investigated area.

Caudal area 46v

Concerning caudal 46v, decoding analysis shows that this area is characterized by a pattern of Condition coding that is shared between a phase encompassing the final part of the Decision and the initial part of the Behavioral response periods and the Cue/Presentation periods. A similar pattern has been described in our previous work (Rozzi et al., 2023) in which we proposed that this pattern indicates that the presented cue and object are already coded in terms of behavioral outputs ('pragmatic' hypothesis, see (Rozzi et al., 2023)). Looking at the mean population response, task-related neurons of Caudal 46v show a preference for the Action condition during cue and object appearance and an inhibition when the eyes are free to move (after reward delivery in both conditions and, though less evident, around object holding in the Action condition). Considering that this area is strongly connected with oculomotor centers (Borra et al., 2015; Gerbella et al., 2013), this inhibition suggests that the prospective coding observed in the decoding analysis could be linked to the oculomotor control.

Middle area 46v

Considering middle 46v, the decoding analysis shows a very stable representation of the Condition from the Presentation period onwards, and dPCA shows that this area is characterized by a very strong differentiation between Conditions, especially in the final phase of the task. In addition, the mean population response observed in this area revealed a clear preference for the Action condition from object presentation to the end of the task. The same pattern of activity has been described in our previous work (Rozzi et al., 2023), when considering the population of neurons recorded in the whole VLPF showing a preference for the Action condition. Altogether,

these data indicate that neurons of middle 46v encode information related to the presented visual stimuli in terms of the subsequent goal to be achieved rather than in purely visual terms. In other words, neurons of middle 46v encode objects in pragmatic terms, namely as predictions of the critical events signaling the behavioral outcome (e.g., for example, taking possession and pulling the object and reward delivery, 'pragmatic' hypothesis; (Rozzi et al., 2023)).

These results are in line with electrophysiological studies showing that prefrontal neurons encoding the behavioral output during the execution of a motor task are located mainly in the intermediate portion of area 46v (Hoshi et al., 1998; Rainer et al., 1999; Simone et al., 2015; Tanila et al., 1993), as well as with its strong parietal and premotor connectivity (Barbas & Mesulam, 1985; Gerbella et al., 2013). These connections could provide middle 46v with the motor signals and sensory (somatosensory and visual) information necessary for the on-line control of behavior and for monitoring the achievement of the final action goal.

Caudal area 12r

In Caudal 12r, Condition decoding reveals a temporally stable pattern that emerges with object presentation and persists until the final phases of the task, closely resembling the generalization profile observed for Object decoding. This similarity suggests that Condition-related information, in this area, is represented in a format closely tied to object-related encoding. Given the above-mentioned strong involvement of this area in processing passive visual stimuli, we propose that the coding of contextual information observed in the Visuo-Motor task reflects predominantly a visual coding. This interpretation is further supported by anatomical evidence showing that Caudal 12r has extra-prefrontal connections primarily limited to high order inferotemporal areas (Borra et al., 2011).

Middle area 12r

Concerning middle 12r, Condition decoding revealed a shared representation of this factor between Decision and Cue periods. A similar pattern was identified by Rozzi and coworkers (Rozzi et al., 2023) when analyzing the population of Cue-related neurons showing a preference for the Inaction condition. This suggests that cue appearance in the Inaction condition is coded in terms of

the expected feedback signaling goal achievement (i.e. withholding hand movements till reward). Altogether, these findings suggest that middle area 12r may be primarily involved in exploiting visual contextual information to guide behavior. This interpretation is supported by the strong connections of this area with high order inferotemporal regions, and with the parieto-premotor circuit involved in hand grasping actions (Borra et al., 2011; Murata et al., 2000; Sakata et al., 1995).

Area 45A

Area 45A is the only sector in which Cue responses are more represented than those to the other periods of the task. In addition, the mean population response is strongly enhanced during cue and object presentation and slightly inhibited during fixation maintenance (Behavioral response period of the Inaction condition). These findings are in line with the strong connections of this area with parietal and frontal areas and subcortical centers involved in oculomotion (Gerbella et al., 2010).

The nonspecific visual responses of neurons of this area to behaviorally relevant information could be related to possible attentional processes, in line with a series of observation indicating a specific involvement of this region in attention-related functions linked to the visual search of specific targets (Bichot et al., 2015; Wardak et al., 2010).

Rostral sector

The rostral sector of the investigated region of VLPF is much less responsive to the tasks employed in this work. This does not appear to depend on a low numerosity of recorded neurons, since this is quite similar to that of the other investigated areas. The low responsiveness could be due to the fact that our tasks were not able to probe the specific functions of this region. This negative result, however, allow us to define a clear border between the above-described areas and this rostral territory.

The time course of the population response of this area is characterized, in the Visuo-Motor task, by an interesting functional feature: the activity is suppressed during the whole task unfolding, in both Action and Inaction conditions, except for two excitatory peaks in correspondence of stimuli

presentation. This inhibition could be interpreted in light of a large corpus of literature showing that the rostral prefrontal cortex is deeply involved in several operations, such as coding behavioral rules based on past episodic information, coding self-generated decisions and storing conscious action plans (Koechlin et al., 2003; Nee & D'Esposito, 2016, 2017; Soon et al., 2008; Tsujimoto et al., 2010). As the task strongly depends on a clearly defined and immediately available context and is well learned by monkeys, the VLPF areas active during both Action and Inaction conditions could in the meantime inhibit the activity of rostral VLPF. This explanation is corroborated by the known strong intra-prefrontal connectivity of the rostral VLPF sector with more posterior VLPF regions (Borra et al., 2011; Gerbella et al., 2013).

4.6 Limitations and further developments

Usually, neurophysiological studies test functions of cortical regions by using a task specifically aimed to evaluate the effect of few variables and by limiting the analysis to task-related neurons. In this paper, we employed three different tasks to better evaluate multiple functional variables on the same neurons. Furthermore, although in the main text we present the properties of task-related neurons, we also demonstrate that the results are confirmed, for each area, in the whole population of recorded neurons (see Supporting information). Thus, we can infer that the properties of the population of task-related neurons are representative of those of the whole investigated region within the studied functions.

However, the present work has, as a main limitation, the fact that the employed tasks only partially allowed us to characterize the functions of 45A and of the rostral sector of VLPF. Further studies could allow to better define the properties of these two cortical sectors, by verifying their response to other types of sensory stimuli (e.g. acoustic, somatosensory or multimodal), by assessing their role in high level guidance of oculomotor behavior, and in the processing of abstract information stored in episodic memory.

The types of motor behavior studied in this work, i.e. grasping objects and withholding actions, are daily performed also by humans, therefore our results could be important for verifying whether a modular organization of cognitive-motor functions, similar to that here described in the monkey VLPF, is present also in our species. Interestingly, in many prefrontal neuropsychological syndromes, such as utilization behavior, echopraxia, and anarchic hand syndrome, the impairment of cognitive aspects is intrinsically linked to the motor ones (De Renzi et al., 1996; Lhermitte, 1983, p. 19; Pacherie, 2007). Thus, we believe that the detailed anatomical identification of the prefrontal

areas involved in different aspects of executive functions, such as context-based organization of behavior, will allow a more precise “mapping” of the symptoms of prefrontal syndromes.

5. References

Asaad, W. F., Rainer, G., & Miller, E. K. (1998). Neural activity in the primate prefrontal cortex during associative learning. *Neuron*, *21*(6), 1399–1407. https://doi.org/10.1016/s0896-6273(00)80658-3

Assem, M., Glasser, M. F., Van Essen, D. C., & Duncan, J. (2020). A Domain-General Cognitive Core Defined in Multimodally Parcellated Human Cortex. *Cerebral Cortex*, *30*(8), 4361–4380. https://doi.org/10.1093/cercor/bhaa023

Averbeck, B. B., Chafee, M. V., Crowe, D. A., & Georgopoulos, A. P. (2002). Parallel processing of serial movements in prefrontal cortex. *Proceedings of the National Academy of Sciences*, *99*(20), 13172–13177. https://doi.org/10.1073/pnas.162485599

Blinkov, S. M., & Glezer, I. I. (1968). *The Human Brain in Figures and Tables: A Quantitative Handbook*. Basic Books. https://books.google.it/books?id=eLJqAAAAMAAJ

Boch, R. A., & Goldberg, M. E. (1989). Participation of prefrontal neurons in the preparation of visually guided eye movements in the rhesus monkey. *Journal of Neurophysiology*, *61*(5), 1064–1084. https://doi.org/10.1152/jn.1989.61.5.1064

Borra, E., Gerbella, M., Rozzi, S., & Luppino, G. (2011). Anatomical evidence for the involvement of the macaque ventrolateral prefrontal area 12r in controlling goal-directed actions. *The Journal of Neuroscience : The Official Journal of the Society for Neuroscience*, *31*(34), 12351–12363. https://doi.org/10.1523/JNEUROSCI.1745-11.2011

Borra, E., Gerbella, M., Rozzi, S., & Luppino, G. (2015). Projections from caudal ventrolateral prefrontal areas to brainstem preoculomotor structures and to Basal Ganglia and cerebellar oculomotor loops in the macaque. *Cerebral Cortex (New York, N.Y. : 1991)*, *25*(3), 748–764. https://doi.org/10.1093/cercor/bht265

Borra, E., Gerbella, M., Rozzi, S., & Luppino, G. (2017). The macaque lateral grasping network: A neural substrate for generating purposeful hand actions. *Neuroscience and Biobehavioral Reviews*, *75*, 65–90. https://doi.org/10.1016/j.neubiorev.2017.01.017

Borra, E., Gerbella, M., Rozzi, S., Tonelli, S., & Luppino, G. (2014). Projections to the superior colliculus from inferior parietal, ventral premotor, and ventrolateral prefrontal areas involved in controlling goal-directed hand actions in the macaque. *Cerebral Cortex (New York, N.Y. : 1991)*, *24*(4), 1054–1065. https://doi.org/10.1093/cercor/bhs392

Boussaoud, D., & Wise, S. P. (1993). Primate frontal cortex: Neuronal activity following attentional versus intentional cues. *Experimental Brain Research*, *95*(1), 15–27. https://doi.org/10.1007/BF00229650

Brodmann, K. (1909). *Vergleichende Lokalisationslehre der Grosshirnrinde: In ihren Prinzipien dargestellt auf Grund des Zellenbaues* (2nd unveränderte Aufl.). Barth.

Bruni, S., Giorgetti, V., Bonini, L., & Fogassi, L. (2015). Processing and Integration of Contextual Information in Monkey Ventrolateral Prefrontal Neurons during Selection and Execution of Goal-Directed Manipulative Actions. *Journal of Neuroscience*, *35*(34), 11877–11890. https://doi.org/10.1523/JNEUROSCI.1938-15.2015

Carlén, M. (2017). What constitutes the prefrontal cortex? *Science*, *358*(6362), 478–482. https://doi.org/10.1126/science.aan8868

Chafee, M. V., & Goldman-Rakic, P. S. (2000). Inactivation of parietal and prefrontal cortex reveals interdependence of neural activity during memory-guided saccades. *Journal of Neurophysiology*, *83*(3), 1550–1566. https://doi.org/10.1152/jn.2000.83.3.1550

Constantinidis, C., & Procyk, E. (2004). The primate working memory networks. *Cognitive, Affective, & Behavioral Neuroscience*, *4*(4), 444–465. https://doi.org/10.3758/CABN.4.4.444

Constantinidis, C., & Qi, X.-L. (2018). Representation of Spatial and Feature Information in the Monkey Dorsal and Ventral Prefrontal Cortex. *Frontiers in Integrative Neuroscience*, *12*. https://doi.org/10.3389/fnint.2018.00031

Crittenden, B. M., & Duncan, J. (2014). Task difficulty manipulation reveals multiple demand activity but no frontal lobe hierarchy. *Cerebral Cortex*, *24*(2), 532–540. https://doi.org/10.1093/cercor/bhs333

Desimone, R., & Duncan, J. (1995). Neural Mechanisms of Selective Visual Attention. *Annual Review of Neuroscience*, *18*(Volume 18, 1995), 193–222. https://doi.org/10.1146/annurev.ne.18.030195.001205

Duncan, J. (2001). An adaptive coding model of neural function in prefrontal cortex. *Nature Reviews Neuroscience*, *2*(11), 820–829. https://doi.org/10.1038/35097575

Duncan, J. (2010). The multiple-demand (MD) system of the primate brain: Mental programs for intelligent behaviour. *Trends in Cognitive Sciences*, *14*(4), 172–179. https://doi.org/10.1016/j.tics.2010.01.004

Duncan, J., & Owen, A. M. (2000). Common regions of the human frontal lobe recruited by diverse cognitive demands. *Trends in Neurosciences*, *23*(10), 475–483. https://doi.org/10.1016/S0166-2236(00)01633-7

Everling, S., Tinsley, C. J., Gaffan, D., & Duncan, J. (2002). Filtering of neural signals by focused attention in the monkey prefrontal cortex. *Nature Neuroscience*, *5*(7), 671–676. https://doi.org/10.1038/nn874

Freedman, D. J., Riesenhuber, M., Poggio, T., & Miller, E. K. (2001). Categorical representation of visual stimuli in the primate prefrontal cortex. *Science (New York, N.Y.)*, *291*(5502), 312–316. https://doi.org/10.1126/science.291.5502.312

Funahashi, S., & Andreau, J. M. (2013). Prefrontal cortex and neural mechanisms of executive function. *Journal of Physiology, Paris*, *107*(6), 471–482. https://doi.org/10.1016/j.jphysparis.2013.05.001

Funahashi, S., Bruce, C. J., & Goldman-Rakic, P. S. (1989). Mnemonic coding of visual space in the monkey's dorsolateral prefrontal cortex. *Journal of Neurophysiology*, *61*(2), 331–349. https://doi.org/10.1152/jn.1989.61.2.331

Funahashi, S., Bruce, C. J., & Goldman-Rakic, P. S. (1991). Neuronal activity related to saccadic eye movements in the monkey's dorsolateral prefrontal cortex. *Journal of Neurophysiology*, *65*(6), 1464–1483. https://doi.org/10.1152/jn.1991.65.6.1464

Funahashi, S., Inoue, M., & Kubota, K. (1993). Delay-related activity in the primate prefrontal cortex during sequential reaching tasks with delay. *Neuroscience Research*, *18*(2), 171–175. https://doi.org/10.1016/0168-0102(93)90019-M

Fuster, J. M. (2015). Neurophysiology. In *The Prefrontal Cortex* (pp. 237–308). Elsevier. https://doi.org/10.1016/B978-0-12-407815-4.00006-4

Fuster, J. M., & Alexander, G. E. (1971). Neuron Activity Related to Short-Term Memory. *Science*, *173*(3997), 652–654. https://doi.org/10.1126/science.173.3997.652

Gerbella, M., Belmalih, A., Borra, E., Rozzi, S., & Luppino, G. (2007). Multimodal architectonic subdivision of the caudal ventrolateral prefrontal cortex of the macaque monkey. *Brain Structure and Function*, *212*(3–4), 269–301. https://doi.org/10.1007/s00429-007-0158-9

Gerbella, M., Belmalih, A., Borra, E., Rozzi, S., & Luppino, G. (2010). Cortical Connections of the Macaque Caudal Ventrolateral Prefrontal Areas 45A and 45B. *Cerebral Cortex*, *20*(1), 141–168. https://doi.org/10.1093/cercor/bhp087

Gerbella, M., Borra, E., Mangiaracina, C., Rozzi, S., & Luppino, G. (2016). Corticostriate Projections from Areas of the "Lateral Grasping Network": Evidence for Multiple Hand-Related Input Channels. *Cerebral Cortex*, *26*(7), 3096–3115. https://doi.org/10.1093/cercor/bhv135

Gerbella, M., Borra, E., Tonelli, S., Rozzi, S., & Luppino, G. (2013). Connectional heterogeneity of the ventral part of the macaque area 46. *Cerebral Cortex (New York, N.Y. : 1991)*, *23*(4), 967–987. https://doi.org/10.1093/cercor/bhs096

Gerbella, M., Rozzi, S., & Rizzolatti, G. (2017). The extended object-grasping network. *Experimental Brain Research*, *235*(10), 2903–2916. https://doi.org/10.1007/s00221-017-5007-3

Hoshi, E., Shima, K., & Tanji, J. (1998). Task-Dependent Selectivity of Movement-Related Neuronal Activity in the Primate Prefrontal Cortex. *Journal of Neurophysiology*, *80*(6), 3392–3397. https://doi.org/10.1152/jn.1998.80.6.3392

Hoshi, E., Shima, K., & Tanji, J. (2000). Neuronal Activity in the Primate Prefrontal Cortex in the Process of Motor Selection Based on Two Behavioral Rules. *Journal of Neurophysiology*, *83*(4), 2355–2373. https://doi.org/10.1152/jn.2000.83.4.2355

Ichihara-Takeda, S., & Funahashi, S. (2007). Activity of primate orbitofrontal and dorsolateral prefrontal neurons: Task-related activity during an oculomotor delayed-response task. *Experimental Brain Research*, *181*(3), 409–425. https://doi.org/10.1007/s00221-007-0941-0

Kadohisa, M., Kusunoki, M., Mitchell, D. J., Bhatia, C., Buckley, M. J., & Duncan, J. (2023). Frontal and temporal coding dynamics in successive steps of complex behavior. *Neuron*, *111*(3), 430-443.e3. https://doi.org/10.1016/j.neuron.2022.11.004

Katsuki, F., & Constantinidis, C. (2014). Bottom-Up and Top-Down Attention: Different Processes and Overlapping Neural Systems. *The Neuroscientist*, *20*(5), 509–521. https://doi.org/10.1177/1073858413514136

Kubota, K., & Funahashi, S. (1982). Direction-specific activities of dorsolateral prefrontal and motor cortex pyramidal tract neurons during visual tracking. *Journal of Neurophysiology*, *47*(3), 362–376. https://doi.org/10.1152/jn.1982.47.3.362

Kubota, K., & Niki, H. (1971). Prefrontal cortical unit activity and delayed alternation performance in monkeys. *Journal of Neurophysiology*, *34*(3), 337–347. https://doi.org/10.1152/jn.1971.34.3.337

Levy, R., & Goldman-Rakic, P. S. (2000). Segregation of working memory functions within the dorsolateral prefrontal cortex. *Experimental Brain Research*, *133*(1), 23–32. https://doi.org/10.1007/s002210000397

Miller, E. K., & Cohen, J. D. (2001). An Integrative Theory of Prefrontal Cortex Function. *Annual Review of Neuroscience*, *24*(1), 167–202. https://doi.org/10.1146/annurev.neuro.24.1.167

Miller, E. K., Erickson, C. A., & Desimone, R. (1996). Neural Mechanisms of Visual Working Memory in Prefrontal Cortex of the Macaque. *The Journal of Neuroscience*, *16*(16), 5154–5167. https://doi.org/10.1523/JNEUROSCI.16-16-05154.1996

Miller, E. K., Freedman, D. J., & Wallis, J. D. (2002). The prefrontal cortex: Categories, concepts and cognition. *Philosophical Transactions of the Royal Society of London. Series B, Biological Sciences*, *357*(1424), 1123–1136. https://doi.org/10.1098/rstb.2002.1099

Miller, E. K., Lundqvist, M., & Bastos, A. M. (2018). Working Memory 2.0. *Neuron*, *100*(2), 463–475. https://doi.org/10.1016/j.neuron.2018.09.023

Mishkin, M., & Manning, F. J. (1978). Non-spatial memory after selective prefrontal lesions in monkeys. *Brain Research*, *143*(2), 313–323. https://doi.org/10.1016/0006-8993(78)90571-1

Muhammad, R., Wallis, J. D., & Miller, E. K. (2006). A Comparison of Abstract Rules in the Prefrontal Cortex, Premotor Cortex, Inferior Temporal Cortex, and Striatum. *Journal of Cognitive Neuroscience*, *18*(6), 974–989. https://doi.org/10.1162/jocn.2006.18.6.974

Nelissen, K., Luppino, G., Vanduffel, W., Rizzolatti, G., & Orban, G. A. (2005). Observing Others: Multiple Action Representation in the Frontal Lobe. *Science*, *310*(5746), 332–336. https://doi.org/10.1126/science.1115593

Niki, H. (1974). Differential activity of prefrontal units during right and left delayed response trials. *Brain Research*, *70*(2), 346–349. https://doi.org/10.1016/0006-8993(74)90324-2

Niki, H., & Watanabe, M. (1976). Prefrontal unit activity and delayed response: Relation to cue location *versus* direction of response. *Brain Research*, *105*(1), 79–88. https://doi.org/10.1016/0006-8993(76)90924-0

Passingham, R. E., Toni, I., & Rushworth, M. F. S. (2000). Specialisation within the prefrontal cortex: The ventral prefrontal cortex and associative learning. *Experimental Brain Research*, *133*(1), 103–113. https://doi.org/10.1007/s002210000405

Petrides, M., & Pandya, D. N. (1999). Dorsolateral prefrontal cortex: Comparative cytoarchitectonic analysis in the human and the macaque brain and corticocortical connection patterns. *The European Journal of Neuroscience*, *11*(3), 1011–1036. https://doi.org/10.1046/j.1460-9568.1999.00518.x

Petrides, M., & Pandya, D. N. (2002). Comparative cytoarchitectonic analysis of the human and the macaque ventrolateral prefrontal cortex and corticocortical connection patterns in the monkey. *The European Journal of Neuroscience*, *16*(2), 291–310. https://doi.org/10.1046/j.1460-9568.2001.02090.x

Petrides, M., Tomaiuolo, F., Yeterian, E. H., & Pandya, D. N. (2011). *The prefrontal cortex: Comparative architectonic organization in the human and the macaque monkey brains*. https://doi.org/10.1016/j.cortex.2011.07.002

Quintana, J., & Fuster, J. M. (1992). Mnemonic and predictive functions of cortical neurons in a memory task. *Neuroreport*, *3*(8), 721–724. https://doi.org/10.1097/00001756-199208000-00018

Riley, M. R., Qi, X.-L., & Constantinidis, C. (2017). Functional specialization of areas along the anterior-posterior axis of the primate prefrontal cortex. *Cerebral Cortex (New York, N.Y. : 1991)*, *27*(7), 3683–3697. https://doi.org/10.1093/cercor/bhw190

Romanski, L. M. (2004). Domain specificity in the primate prefrontal cortex. *Cognitive, Affective & Behavioral Neuroscience*, *4*(4), 421–429. https://doi.org/10.3758/cabn.4.4.421

Romanski, L. M. (2007). Representation and integration of auditory and visual stimuli in the primate ventral lateral prefrontal cortex. *Cerebral Cortex (New York, N.Y. : 1991)*, *17 Suppl 1*(Suppl 1), i61-9. https://doi.org/10.1093/cercor/bhm099

Romanski, L. M., & Averbeck, B. B. (2009). The Primate Cortical Auditory System and Neural Representation of Conspecific Vocalizations. *Annual Review of Neuroscience*, *32*, 315–346. https://doi.org/10.1146/annurev.neuro.051508.135431

Rozzi, S., Bimbi, M., Gravante, A., Simone, L., & Fogassi, L. (2021). Visual response of ventrolateral prefrontal neurons and their behavior-related modulation. *Scientific Reports*, *11*(1), 10118. https://doi.org/10.1038/s41598-021-89500-0

Rozzi, S., Gravante, A., Basile, C., Cappellaro, G., Gerbella, M., & Fogassi, L. (2023). Ventrolateral prefrontal neurons of the monkey encode instructions in the 'pragmatic' format of the associated behavioral outcomes. *Progress in Neurobiology*, *229*, 102499. https://doi.org/10.1016/j.pneurobio.2023.102499

Saga, Y., Iba, M., Tanji, J., & Hoshi, E. (2011). Development of multidimensional representations of task phases in the lateral prefrontal cortex. *Journal of Neuroscience*, *31*(29), 10648–10665. https://doi.org/10.1523/JNEUROSCI.0988-11.2011

Saito, N., Mushiake, H., Sakamoto, K., Itoyama, Y., & Tanji, J. (2005). Representation of Immediate and Final Behavioral Goals in the Monkey Prefrontal Cortex during an Instructed Delay Period. *Cerebral Cortex*, *15*(10), 1535–1546. https://doi.org/10.1093/cercor/bhi032

Saleem, K. S., Miller, B., & Price, J. L. (2014). Subdivisions and connectional networks of the lateral prefrontal cortex in the macaque monkey. *The Journal of Comparative Neurology*, *522*(7), 1641–1690. https://doi.org/10.1002/cne.23498

Seger, C. A., & Miller, E. K. (2010). Category learning in the brain. *Annual Review of Neuroscience*, *33*, 203–219. https://doi.org/10.1146/annurev.neuro.051508.135546

Semendeferi, K., Lu, A., Schenker, N., & Damasio, H. (2002). Humans and great apes share a large frontal cortex. *Nature Neuroscience*, *5*(3), 272–276. https://doi.org/10.1038/nn814

Shima, K., Isoda, M., Mushiake, H., & Tanji, J. (2007). Categorization of behavioural sequences in the prefrontal cortex. *Nature*, *445*(7125), 315–318. https://doi.org/10.1038/nature05470

Simone, L., Bimbi, M., Rodà, F., Fogassi, L., & Rozzi, S. (2017). Action observation activates neurons of the monkey ventrolateral prefrontal cortex. *Scientific Reports*, *7*. https://doi.org/10.1038/srep44378

Simone, L., Rozzi, S., Bimbi, M., & Fogassi, L. (2015). Movement-related activity during goal-directed hand actions in the monkey ventrolateral prefrontal cortex. *The European Journal of Neuroscience*, *42*(11), 2882–2894. https://doi.org/10.1111/ejn.13040

Smaers, J. B., Steele, J., Case, C. R., Cowper, A., Amunts, K., & Zilles, K. (2011). *Primate Prefrontal Cortex Evolution: Human Brains Are the Extreme of a Lateralized Ape Trend*. https://doi.org/10.1159/000323671

Somel, M., Franz, H., Yan, Z., Lorenc, A., Guo, S., Giger, T., Kelso, J., Nickel, B., Dannemann, M., Bahn, S., Webster, M. J., Weickert, C. S., Lachmann, M., Pääbo, S., & Khaitovich, P. (2009). Transcriptional neoteny in the human brain. *Proceedings of the National Academy of Sciences of the United States of America*, *106*(14), 5743–5748. https://doi.org/10.1073/pnas.0900544106

Tanila, H., Carlson, S., Linnankoski, I., Lindroos, F., & Kahila, H. (1992). Functional properties of dorsolateral prefrontal cortical neurons in awake monkey. *Behavioural Brain Research*, *47*(2), 169–180. https://doi.org/10.1016/s0166-4328(05)80123-8

Tanji, J., & Hoshi, E. (2008). Role of the Lateral Prefrontal Cortex in Executive Behavioral Control. *Physiological Reviews*, *88*(1), 37–57. https://doi.org/10.1152/physrev.00014.2007

Tsao, D. Y., & Livingstone, M. S. (2008). Mechanisms of face perception. *Annual Review of Neuroscience*, *31*, 411–437. https://doi.org/10.1146/annurev.neuro.30.051606.094238

Van Essen, D. C., Donahue, C. J., & Glasser, M. F. (2018). Development and Evolution of Cerebral and Cerebellar Cortex. *Brain, Behavior and Evolution*, *91*(3), 158–169. https://doi.org/10.1159/000489943

Walker, A. E. (1940). A cytoarchitectural study of the prefrontal area of the macaque monkey. *Journal of Comparative Neurology*, *73*(1), 59–86. https://doi.org/10.1002/cne.900730106

Wallis, J. D., Anderson, K. C., & Miller, E. K. (2001). Single neurons in prefrontal cortex encode abstract rules. *Nature*, *411*(6840), 953–956. https://doi.org/10.1038/35082081

Wang, M., Zhang, H., & Li, B.-M. (2000). Deficit in conditional visuomotor learning by local infusion of bicuculline into the ventral prefrontal cortex in monkeys. *European Journal of Neuroscience*, *12*(10), 3787–3796. https://doi.org/10.1046/j.1460-9568.2000.00238.x

White, I. M., & Wise, S. P. (1999). Rule-dependent neuronal activity in the prefrontal cortex. *Experimental Brain Research*, *126*(3), 315–335. https://doi.org/10.1007/s002210050740

Wilson, F. A. W., Scalaidhe, S. P. Ó., & Goldman-Rakic, P. S. (1993). Dissociation of Object and Spatial Processing Domains in Primate Prefrontal Cortex. *Science*, *260*(5116), 1955–1958. https://doi.org/10.1126/science.8316836

Woolgar, A., Hampshire, A., Thompson, R., & Duncan, J. (2011). Adaptive Coding of Task-Relevant Information in Human Frontoparietal Cortex. *The Journal of Neuroscience*, *31*(41), 14592–14599. https://doi.org/10.1523/JNEUROSCI.2616-11.2011

Yamagata, T., Nakayama, Y., Tanji, J., & Hoshi, E. (2012). Distinct information representation and processing for goal-directed behavior in the dorsolateral and ventrolateral prefrontal cortex and the dorsal premotor cortex. *Journal of Neuroscience*, *32*(37), 12934–12949. https://doi.org/10.1523/JNEUROSCI.2398-12.2012

Yeterian, E. H., Pandya, D. N., Tomaiuolo, F., & Petrides, M. (2012). The cortical connectivity of the prefrontal cortex in the monkey brain. *Cortex; a Journal Devoted to the Study of the Nervous System and Behavior*, *48*(1), 58–81. https://doi.org/10.1016/j.cortex.2011.03.004

Appendix: Supporting Information

Cases	Species	Hemisphere	Area	Injection number	Tracer	Amount
23	Fascicularis	Left	Middle 46v (Skeletomor network)[a]	9	FB 3%	2 × 0.2 µl
26	Nemestrina	Left	45B (Oculomotor network)[a]	38	DY 2%	1 × 0.2 µl
			Caudal 12r (Oculomotor network)[a]	29	FB 3%	1 × 0.2 µl
30	Nemestrina	Right	45B (Oculomotor network)[a]	35	FB 3%	1 × 0.2 µl
36	Fascicularis	Left	45B (Oculomotor network)[a]	39	FB 3%	1 × 0.2 µl
			45A (Oculomotor network)[a]	34	CTBg 1%	1 × 1 µl
		Right	8FEF (Oculomotor network)[a]	16	FR 10%	1 × 1 µl
			45B (Oculomotor network)[a]	37	BDA 10%	1 × 2 µl
37	Rhesus	Left	45A (Oculomotor network)[a]	31	FB 3%	2 × 0.2 µl
			8r (Oculomotor network)[a]	15	CTBr 1%	1 × 1 µl
			8FEF (Oculomotor network)[a]	17	CTBg 1%	1 × 1 µl
		Right	45A (Oculomotor network)[a]	33	BDA 10%	2 × 1 µl
			45B (Oculomotor network)[a]	36	FR 10%	1 × 1 µl
39	Fascicularis	Left	45A (Oculomotor network)[a]	32	FR 10%	2 × 1 µl
43	Rhesus	Left	Rostral 46v (Intraprefrontal)[b]	1	CTBr 1%	1 × 1 µl
			Middle12r (Skeletomor network)[b]	25	FB 3%	1 × 0.2 µl
			Middle 12r (Skeletomor network)[b]	24	DY 2%	1 × 0.2 µl
		Right	Caudal 46v (Oculomotor network)[b]	14	FR 10%	1 × 1 µl
44	Rhesus	Left	Caudal 46v (Oculomotor network)[b]	13	DY 2%	1 × 0.2 µl
			Middle 46v (Skeletomor network)[b]	6	FB 3%	1 × 0.2 µl
		Right	Middle 12r (Skeletomor network)[c]	26	LYD 10%	1 × 1.3 µl
			Middle 12r (Skeletomor network)[c]	27	FR 10%	1 × 1 µl
47	Rhesus	Left	Caudal 12r/Middle12r (Oculomotor/Skeletomor network)[c]	28	LYD 10%	1 × 1.3 µl
			Rostral 12r (Intraprefrontal)[c]	21	BDA 10%	1 × 2 µl
			Rostral 12r (Intraprefrontal)[c]	18	FR 10%	1 × 1 µl
		Right	Rostral 12r (Intraprefrontal)[c]	19	FB 3%	1 × 0.2 µl
			Middle 12r/Rostral 12r (Skeletomor network/ Intraprefrontal)[c]	23	DY 2%	1 × 0.2 µl
48	Rhesus	Left	Caudal 12r (Oculomotor network)[c]	30	LYD 10%	1 × 1.3 µl
		Right	Middle 12r/Rostral 12r (Skeletomor network/ Intraprefrontal)[c]	22	DY 2%	1 × 0.2 µl
			Rostral 12r (Intraprefrontal)[c]	20	FB 3%	1 × 0.2 µl
51	Rhesus	Left	Middle 46v (Skeletomor network)[b]	11	DY 2%	1 × 0.2 µl
			Middle 46v (Skeletomor network)[b]	10	FB 3%	1 × 0.2 µl
			Rostral 46v (Intraprefrontal)[b]	2	BDA 10%	1 × 2 µl
		Right	Rostral 46v (Intraprefrontal)[b]	3	CTBg 1%	1 × 1 µl
52	Rhesus	Left	Middle 46v (Skeletomor network)[b]	7	FB 3%	1 × 0.2 µl

	Right	Middle 46v (Skeletomor network)[b]	5	DY 2%	1 × 0.2 µl
		Middle 46v (Skeletomor network)[b]	8	LYD 10%	1 × 1.3 µl
		Caudal 46v/Middle 46v (Oculomotor/Skeletomor network)[b]	12	FR 10%	1 × 1 µl
		Middle 46v (Skeletomor network)[b]	4	BDA 10%	1 × 2 µl

S1 Table. Cases from [a] Gerbella et al. (2010); [b] Gerbella et al. (2013); [c] Borra et al. (2011).

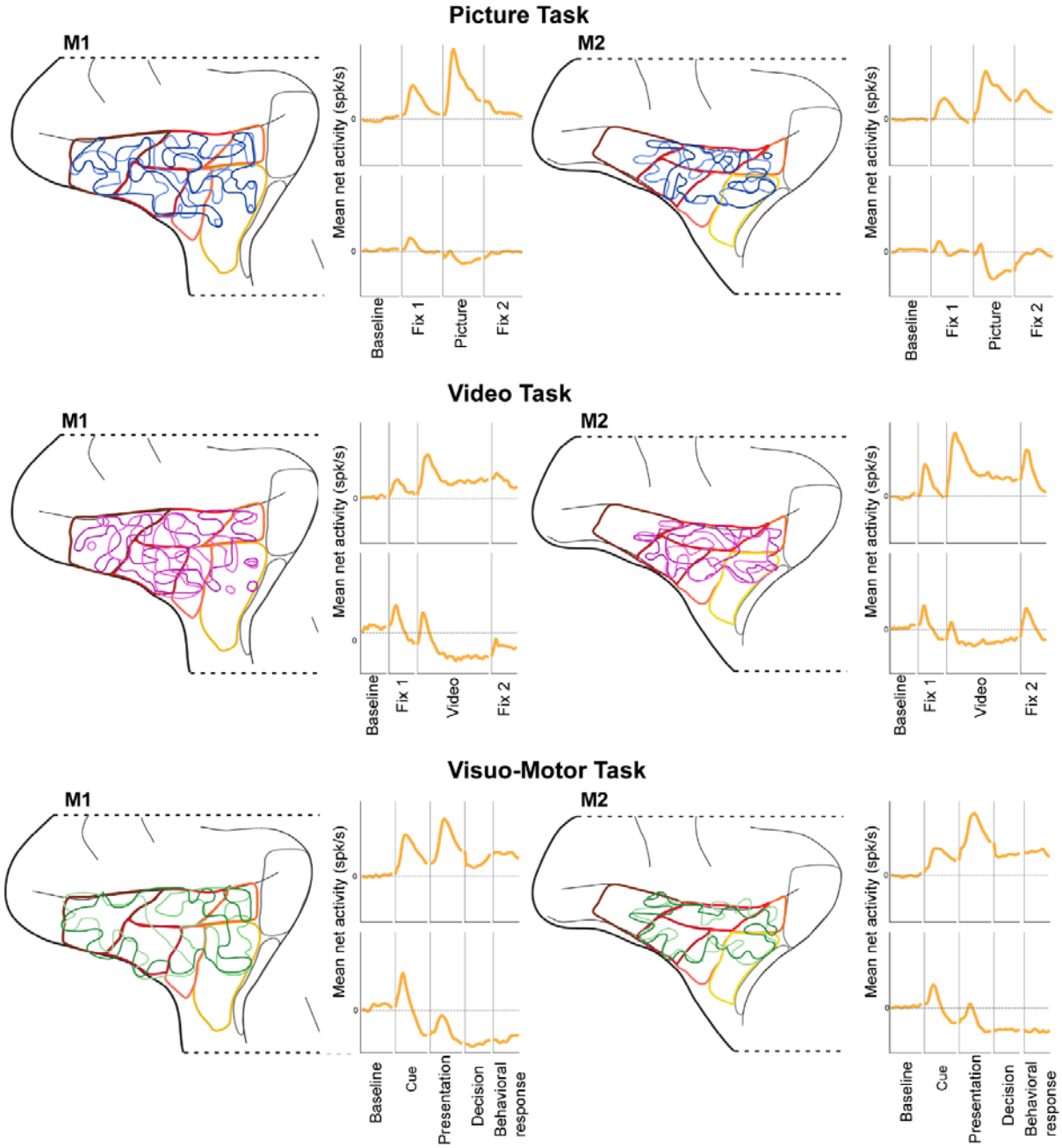

S1 Fig. Spatial distribution and response of task-related neurons belonging to different clusters. Distribution of task-related neurons belonging to each identified cluster in the Picture,

Video, and Visuo-Motor tasks. The distribution of each cluster is represented by colored outlines covering the regions hosting at least two adjacent sites or hosting isolated sites containing more than 31% of neurons belonging to the cluster (see Methods). For each monkey, the temporal profile of the mean baseline-subtracted activity of neurons belonging to each identified cluster is represented on the right of the respective map. The dashed line indicates baseline-level activity. The neuronal activity is aligned on the main task events indicated below each panel of the figure (see Methods for details on the considered periods).

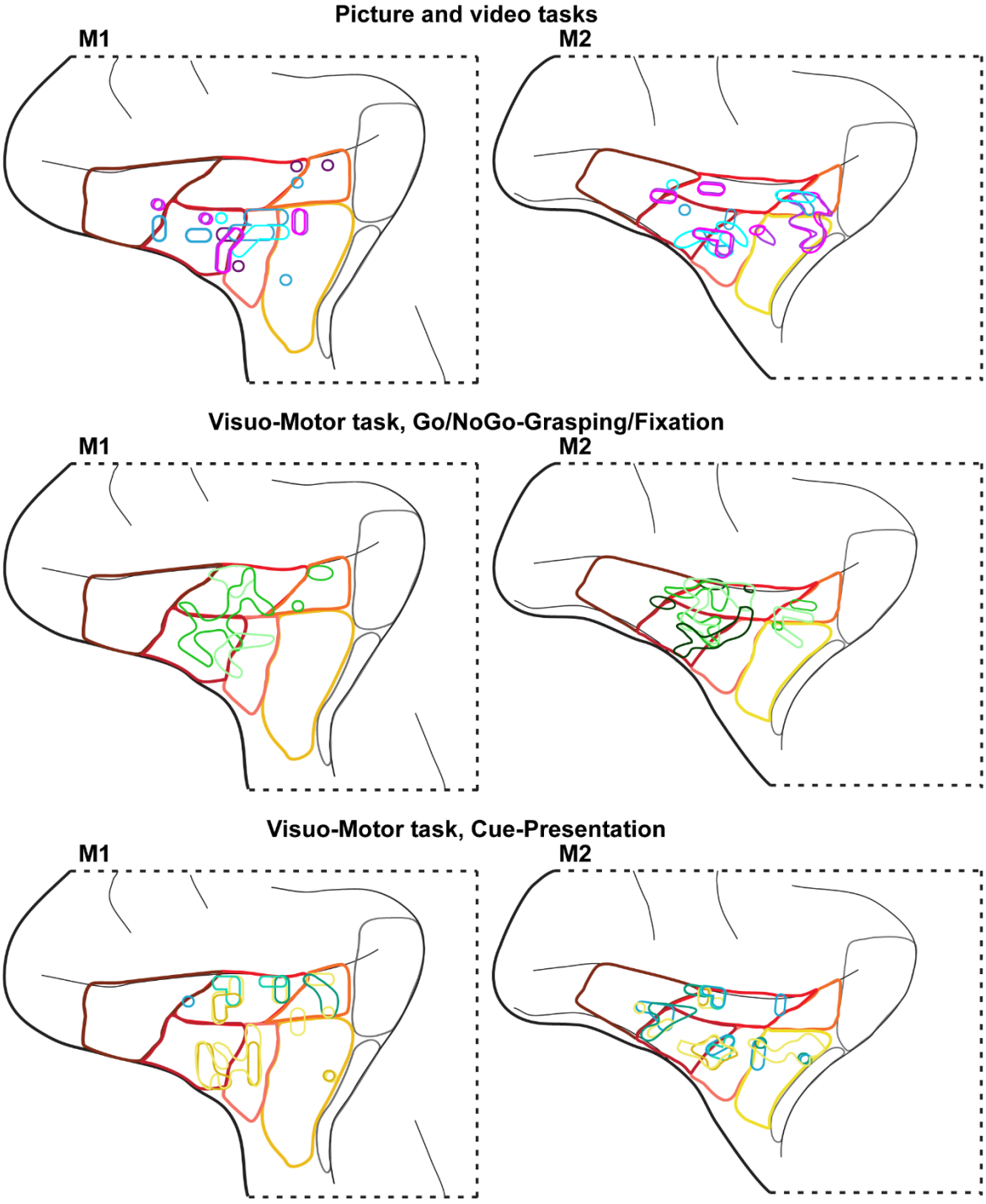

S2 Fig. Spatial distribution of selective neurons belonging to different clusters. Distribution of selective neurons belonging to each cluster identified by considering the Presentation periods of the Picture and Video tasks, the final phase of the Visuo-Motor task, and the Cue and Presentation periods of the Visuo-Motor task. Blue and violet outlines represent the distribution of clusters identified analyzing the Picture and Video task, respectively. Green outlines represent the distribution of clusters identified analyzing the final phases of the Visuo-Motor task. Yellow and light blue outlines represent the distribution of clusters identified analyzing the Cue and Presentation periods of the Visuo-Motor task. Other conventions as in Fig. S1.

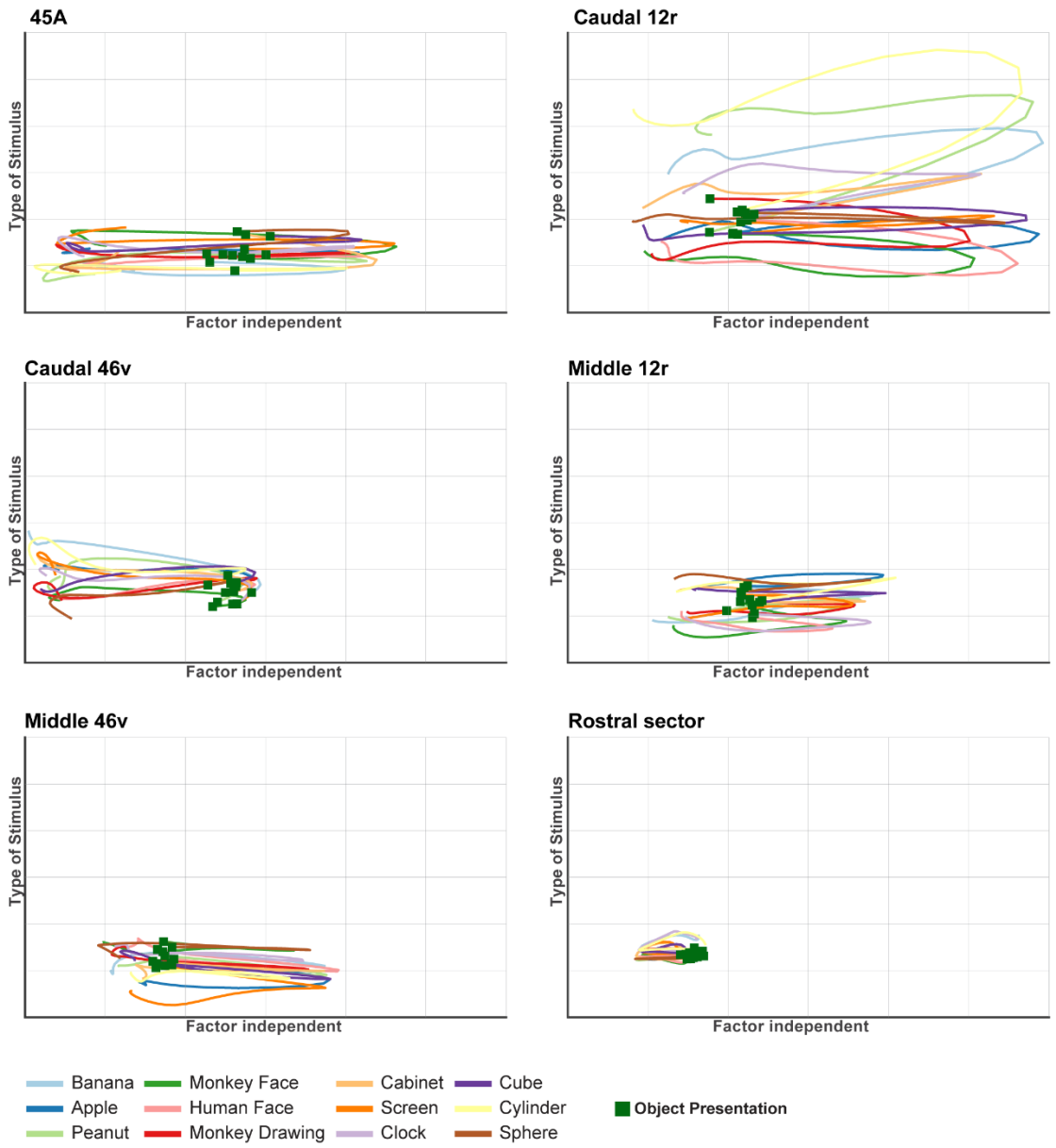

S3 Fig. dPCA trajectories of all recorded neurons of each VLPF area in the Picture task. Each panel depicts the time course of the first Factor-Independent (X axis) and of the first

Type of Stimulus-related (Y axis) principal components plotted together, relative to the population of all neurons recorded in each area. Each colored line corresponds to one of the twelve stimuli presented in the task. Green squares represent the time at which the stimulus presentation occurs.

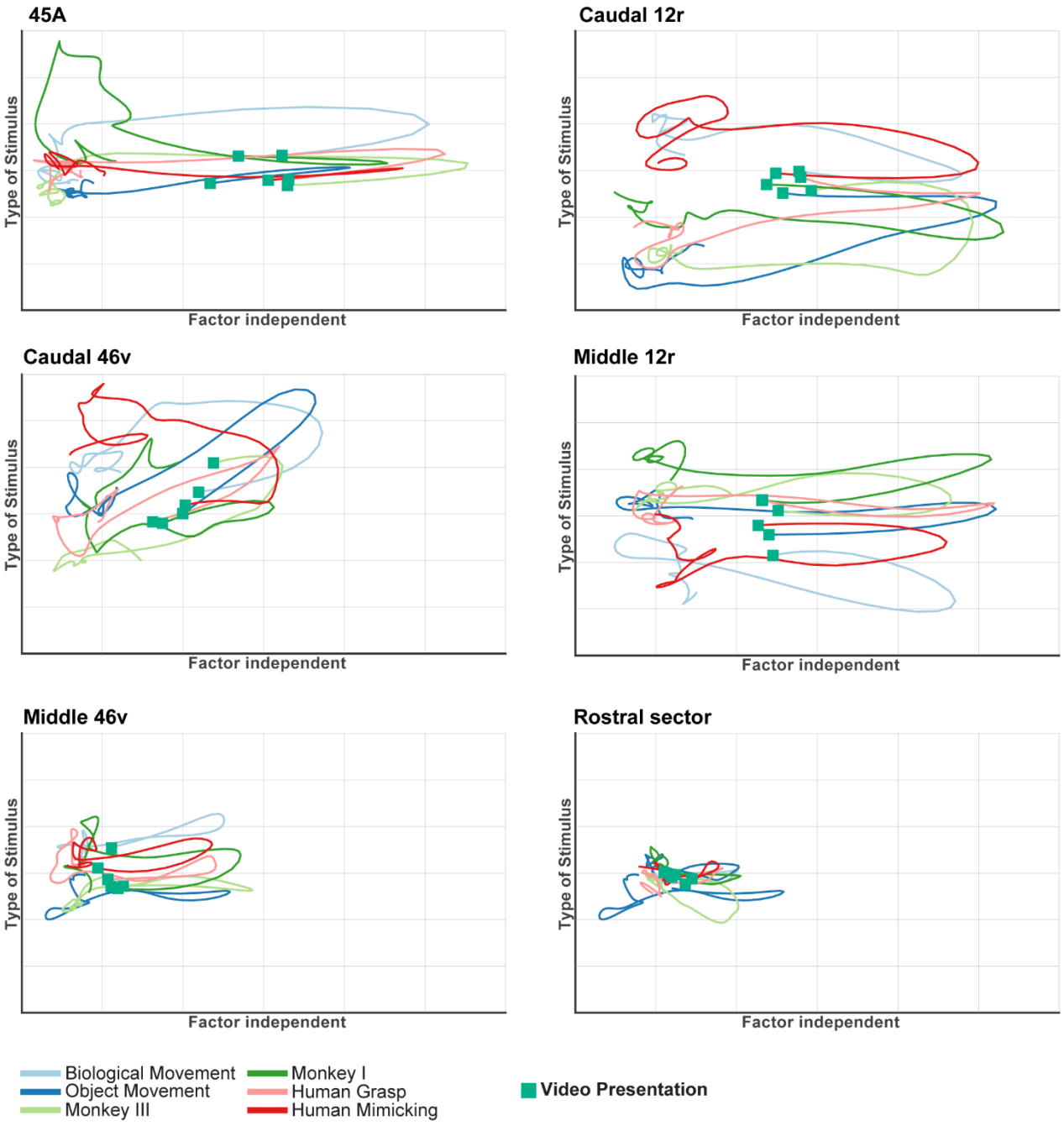

S4 Fig. dPCA trajectories of all recorded neurons of each VLPF area in the Video task. Each panel depicts the time course of the first Factor-Independent (X axis) and of the first Type of Stimulus-related (Y axis) principal components plotted together, relative to the population of all

neurons recorded in each area. Each colored line corresponds to one of the six videos presented in the task. Green squares represent the time at which the stimulus presentation occurs.

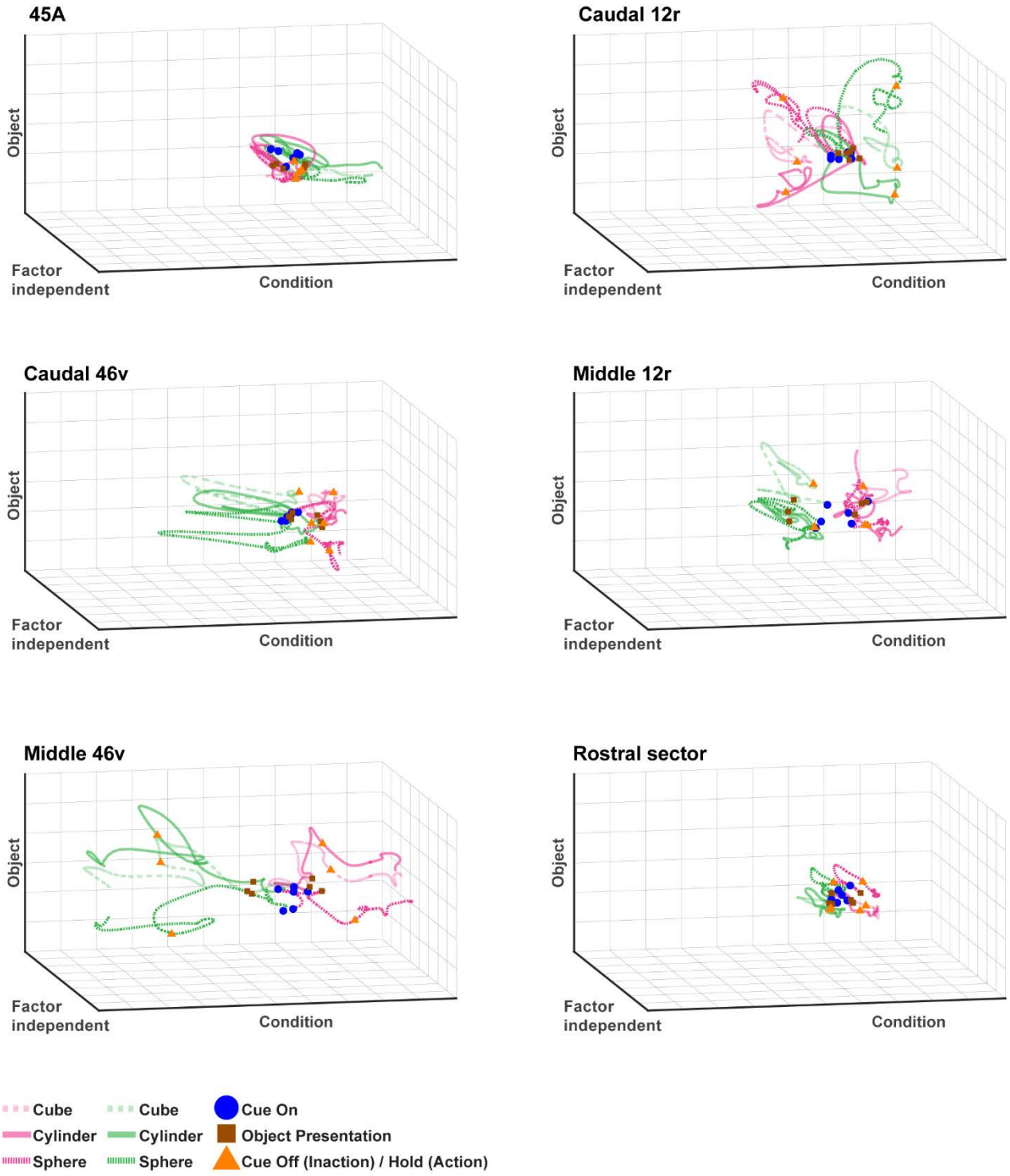

S5 Fig. dPCA trajectories of all recorded neurons of each VLPF area in the Visuo-Motor task. Each panel depicts the time course of the first Condition-related (X axis), of the first Object-related (Y axis) and of the first Factor-Independent (Z axis) principal components, relative to the population of all the neurons recorded in each area. Green and Magenta colored lines

represent Action-related and Inaction-related trajectories, respectively. Continuous and dashed lines correspond to the three objects presented, respectively. Blue circles, brown squares, and orange triangles represent, for each trajectory, the time of cue onset, object presentation, and cue offset, respectively.

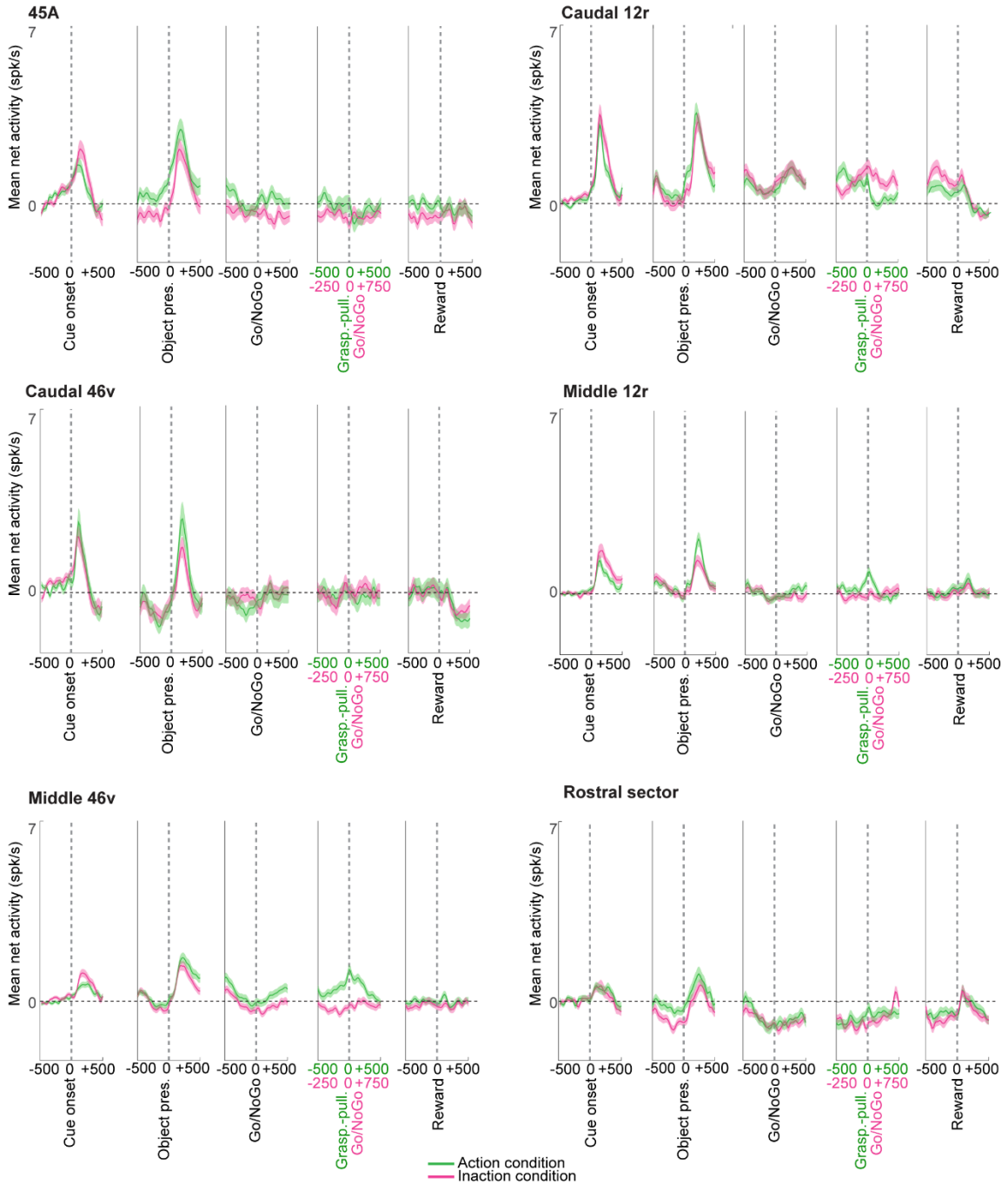

S6 Fig. Mean activity of the whole population of neurons recorded in each area during the Visuo-Motor task. Temporal profile of the mean net activity of the whole population of recorded neurons (including both task-related and non-task-related neurons). Magenta and green

curves indicate the population mean net activity in the Inaction and Action condition, respectively. Other conventions as in Fig 9.

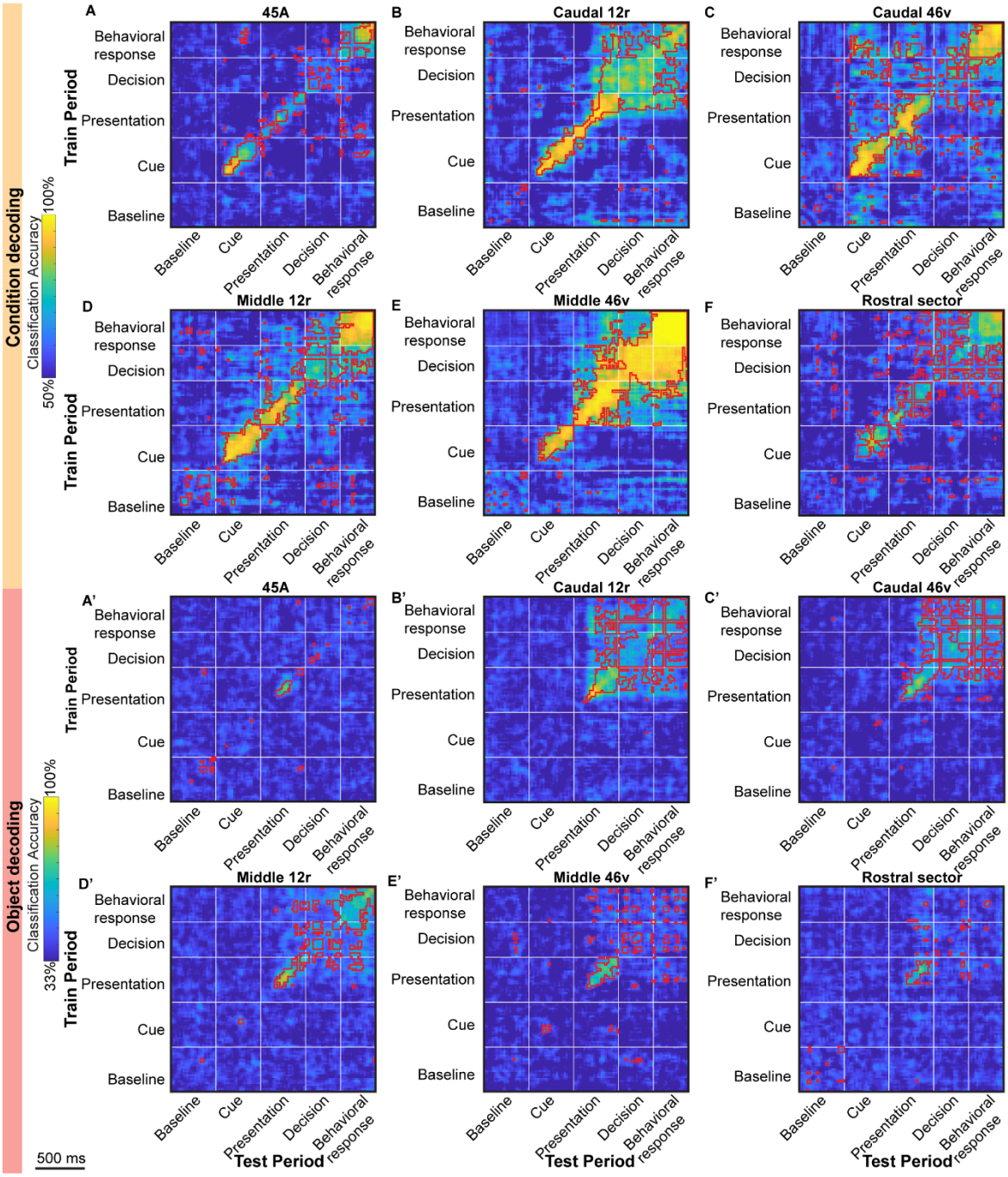

S7 Fig. Cross-temporal decoding of the Condition (A-F) and Object (A'-F') factors of the Visuo-Motor task in the whole population of recorded neurons. For each analysis, the decoding accuracy is computed in bins of 60 ms, sampled at 20 ms intervals. For each plot, the vertical and horizontal lines delimit the considered time periods (see Methods). Other conventions as in Fig 10.